

Hilbert-Geo: Solving Solid Geometric Problems by Neural-Symbolic Reasoning

Ruoran Xu¹, Haoyu Cheng¹, Bin Dong², Qiufeng Wang^{1,†}

¹Xi'an Jiaotong-Liverpool University ²Ricoh Software Research Center Beijing Co.,Ltd.

Abstract

Geometric problem solving, as a typical multimodal reasoning problem, has attracted much attention and made great progress recently, however most of works focus on plane geometry while usually fail in solid geometry due to 3D spatial diagrams and complex reasoning. To bridge this gap, we introduce Hilbert-Geo, the first unified formal language framework for solid geometry, including an extensive predicate library and a dedicated theorem bank. Based on this framework, we propose a Parse2Reason method containing two steps of first parsing then reasoning. In the parsing step, we utilize conditional description language (CDL), a formalized language composed of predicates specifically designed to construct geometric conditions, to represent both problem description (natural text) and solid diagrams (visual image). In the reasoning step, we leverage those formal CDL and the theorem bank to perform relational inference and algebraic computation, generating strictly correct, verifiable, and human-readable reasoning processes. Notably, our proposed Hilbert-Geo is also applicable to plane geometry. To advance geometric reasoning, we curate two expert-annotated dataset SolidFGeo2k and PlaneFGeo3k, which are furnished with geometric formal language annotations, solutions and answers. Extensive experiments show that our proposed method achieves the state-of-the-art (SOTA) performance 77.3% in SolidFGeo2k and 84.1% in MathVerse-Solid (one small subset in MathVerse dedicated to solid geometry), substantially outperforming leading MLLMs, such as Gemini-2.5-pro (54.2% on SolidFGeo2k) and GPT-5 (62.9% on MathVerse-Solid). In addition, our method achieves the SOTA accuracy 80.2% in PlaneFGeo3k, demonstrating the generality of the Hilbert-Geo in geometric reasoning. Our code and datasets will be publicly available.

1. Introduction

“Arithmetic symbols are written figures, and geometric figures are drawn formulas.”—David Hilbert

[†]Corresponding author: qiufeng.wang@xjtlu.edu.cn

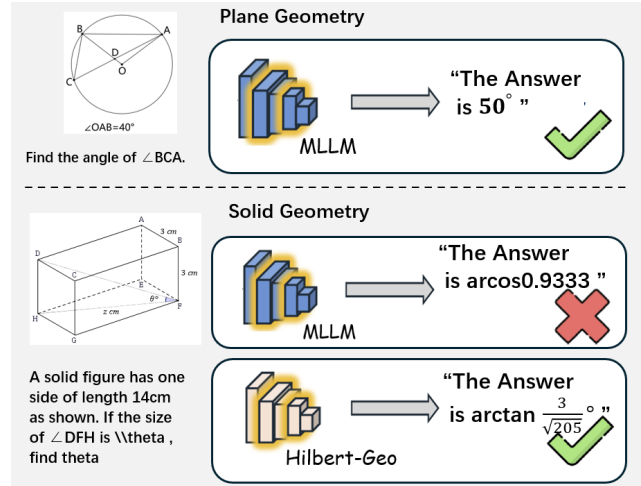


Figure 1. MLLMs struggle with problems in the field of solid geometry (middle) while showing performance in plane geometry problems (top). Our proposed Hilbert-Geo correctly solves this solid geometric problem (bottom).

In recent years, the AI community has made notable breakthroughs in plane geometry, with state-of-the-art systems proficient in solving routine problems and interpreting diagrams, supported by advances in formal reasoning and visual understanding [22]. This progress contrasts sharply with solid geometry, a far more complex and underexplored frontier (See Fig.1) that poses formidable hurdles for MLLMs, manifest in three key aspects: First, solid geometry demands precise grasp of 3D spatial relationships and geometric core concepts [29], requiring reasoning about occluded structures and spatial transformations. This stretches MLLMs’ ability to model abstract spatial logic [5], leading to reasoning errors and knowledge gaps [32]. Second, its inherent multimodality requires sophisticated visual-linguistic grounding: MLLMs must parse text, interpret 2D representations of 3D objects, infer implicit spatial info, and align language with visuals while maintaining cross-modal consistency—often resulting in perception errors and hallucinations [17]. Third, MLLMs are prone to calculation errors in quantitative tasks, further undermining reliability.

Existing solid geometry datasets and benchmarks such

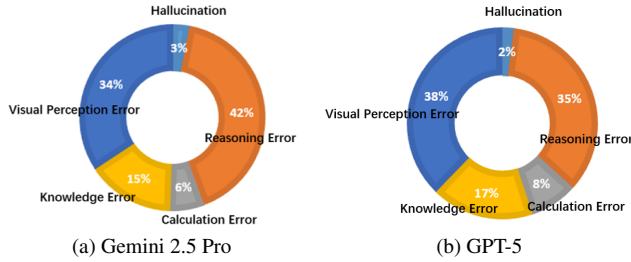


Figure 2. Error distribution in SolidFGeo2k of Gemini and GPT

as MathVerse-Solid [37] and SolidGeo [32] are scattered and flawed. SolidGeo, with 3,000 samples, draws data from single exam question websites, posing potential data leakage risks. Its answers, generated by LLMs, are prone to undetected errors. Moreover, the dataset contains some math modeling and physics problems with low geometric relevance, failing to meet current research and application needs effectively. Additionally, most existing datasets only assess models based on final answers and are prone to data contamination [20]. To mitigate these limitations, we curate an expert-annotated dataset SolidFGeo2k to alleviate the scarcity of high-quality solid reasoning resources and establish a critical benchmark. This dataset is furnished with geometric formal language annotations, detailed reasoning path annotations, and accurate answer labels.

As shown in Fig. 2, we conducted a rigorous fine-grained error analysis on two representative models (Gemini 2.5 Pro [11] and GPT-5 [28]) based on their performance on the SolidFGeo2k dataset. Specifically, we scrutinized all problems that the two models failed to solve correctly, categorizing the resulting errors into five distinct types [29].

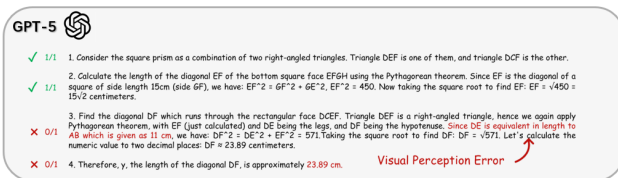


Figure 3. Visual Perception Error for the Problem in Fig. 4

Among all error categories, visual perception errors and reasoning errors are the predominant contributors. For Gemini 2.5 Pro, these two error types collectively account for 76% of the total erroneous cases; for GPT-5, their combined proportion reaches 73%. GPT-5 demonstrates a lower reasoning error rate (35%) in comparison to Gemini 2.5 Pro (42%), while Gemini 2.5 Pro exhibits a lower visual perception error rate (34%) than GPT-5 (38%) (See Fig. 3, an example of visual perception error).

To address these inherent limitations, this study fuses the perceptual capabilities of modern neural networks with the

rigor of formal logic [13]. Building on the foundational theoretical framework of FormalGeo, a plane geometry formalization framework [38], we propose Hilbert-Geo: an explicitly structured formally structured framework [18] designed to tackle the unique challenges of solid geometry. This framework overcomes the core technical bottlenecks intrinsic to three-dimensional reasoning, laying a more robust foundation for solving solid geometric problems.

Comprehensive experimental evaluations demonstrate that Hilbert-Geo achieves state-of-the-art (SOTA) performance, attaining 77.3% accuracy on the SolidFGeo2k benchmark and 84.1% on MathVerse-Solid. This performance significantly outperforms leading multimodal large language models (MLLMs), including Gemini-2.5-Pro (which scored 54.2% on SolidFGeo2k) and GPT-5 (with 62.9% accuracy on MathVerse-Solid).

In summary, our primary contributions are fourfold:

- **Solid Geometry Formal Framework.** We develop a Solid Geometry Predicate Library for precise representation of entities and spatial relationships, complemented by a Solid Geometry Theorem bank.
- **Multimodal Formalization Parser.** We design a pipeline that parses both natural language and visual diagrams, resolving cross-modal ambiguities to ground textual entities in visuals, and translate problems into formal geometric language.
- **Geometry Reasoning Engine.** We introduce an engine for inference on formalized problems, enabling an efficient search of verifiable and human-readable solutions.
- **Two Geometric Datasets.** We construct SolidFGeo2k (solid geometry) and PlaneFGeo3k (plane geometry), both with meticulous formal annotations.

2. Related Work

2.1. Multimodal LLMs in Stereometric Reasoning

While recent years have seen remarkable progress in LLMs and MLLMs, with strong performance across tasks like natural language understanding, visual question answering [8, 12, 16, 23, 33, 34, 40], and multimodal mathematical reasoning (e.g., GPT-5 [27], Gemini [30] surpass average human performance on MathVista [20]), they face critical limitations in stereometric reasoning [15]. First, stereometric knowledge is heterogeneously disseminated across text, graphics, and intuition without a unified formal paradigm [35], yet models rely on informal natural language, leading to ambiguity and failure to encode 3D entities' topological and metric details. Second, existing benchmarks focus mostly on plane geometry [24, 25], neglecting solid geometry's unique spatial and deductive demands. Consequently, LLMs/MLLMs struggle to deliver reliable stereometric reasoning and computations, highlighting an urgent need for targeted advancements.

2.2. Geometric Reasoning with Formalization

The quest for automated geometric problem solving has a rich history. Early systems—Wu’s Method and subsequent algebraic approaches (e.g., Gröbner bases [14], cylindrical algebraic decomposition [2])—offered powerful mechanisms: they solved geometric problems by transforming them into algebraic equations.

Recent work has shifted to formalizing geometric problems for AI. Geometry3K [19] translates problems into formal statements. GeoQA [6] and later geometry reasoning systems such as UniGeo [7] use program-like or expression-tree representations to model problem-solving steps [36]. The FormalGeo system [38] introduced a structured plane geometry formalization approach, with a comprehensive predicate library and theorem system. While these advances plane geometry formalization, their scope remained confined to the plane.

Solid geometric knowledge exhibits formal heterogeneity: it is scattered across textual descriptions, spatial graphics, and abstract intuition, lacking a unified representation paradigm. Meanwhile, spatial relationships are inherently complex, and informal descriptions often cause ambiguous interpretations and reasoning hallucinations—conflicting with mathematical rigor. Worsening these issues, current formalization methods (e.g., plane geometry formalization, general logical systems) cannot effectively capture the topological characteristics and metric relationships of three-dimensional entities (e.g., polyhedrons, spherical surfaces, complex geometries).

3. Solid Geometry Formal Language

3.1. Review of Geometry Formalization Theory

Geometry Formalization theory [38] is centered on the conversion of geometric problems, encompassing known conditions in natural language, problem goals, and geometric diagrams, along with their solution procedures into a unified and precise formal language. It comprises two key components: geometry ontology, which synthesizes core geometric concepts and their interconnections through a knowledge graph focused on Euclidean plane geometry, serving to guide the design of formal systems [3]; geometry representation theory, which investigates the formal expression of geometric knowledge within the framework of consistency theory, guaranteeing the coherence of both components (e.g. formalized diagrams) and processes (e.g. formal descriptions).

3.2. Solid Geometry Formalization Theory

The extension of the formal geometric theoretical framework to the domain of solid geometry is predominantly accomplished via the augmentation of geometric primitives and generalized combinatorial strategies. Furthermore, the

original plane geometric formal category is encapsulated as an entity designated “plane”, which serves as the foundational reference for constructing solid geometric models. Specifically, augmented geometric primitives enable the precise description of basic solid components, while generalized combinatorial strategies include the systematic integration of coverage techniques, clipping techniques, and topological connections, among others. This hierarchical extension strategy not only preserves the completeness of the original plane geometric formalization but also endows the framework with the capability to address complex three-dimensional geometric problems, thereby laying a solid theoretical foundation for subsequent research on solid geometric modeling and automated reasoning. More details in Appendix A.1.

3.3. Predicate Library and Theorem Bank

Predicates act as the fundamental building blocks for characterizing geometric entities. They are integrated into the Geometric Conditional Description Language (CDL), which not only eliminates ambiguities across multimodal representations but also establishes a robust premise for subsequent reasoning tasks [38].

Further elaborations are provided in Appendix A.2. The Solid Predicate Library encompasses 120 predicates, comprising 35 fundamental predicates natively integrated into the solver, along with 20 entity types, 35 entity relationships, and 30 attribute descriptors defined via a dedicated predicate definition language. The formal specification for each predicate includes its name, declaration of point variables, validity check assertions, support for multiple representations, and mechanism for automatic expansion.

Theorems function as the cornerstone of reasoning processes, enabling search-based inference through the self-expansion of geometric entities and the application of theorem-driven deduction [19]. Notably, when defining attributes, symbolic form declarations are also incorporated. The Theorem Bank is an extension of the plane FormalGeo framework, structured into two components: premises and conclusions (detailed in the accompanying table), and encompasses 220 theorems.

4. Datasets of SolidFGeo2k and PlaneFGeo3k

The formalization of natural language geometric descriptions into structured languages like CDL relies heavily on high-quality annotated datasets and benchmarks—serving as both the foundation for model guidance and the benchmark for performance evaluation. Among these, the formally annotated SolidFGeo2k, PlaneFGeo3k datasets are core to this work, providing standardized geometric content, multimodal resources, and CDL formalizations. Below, we first detail these datasets. Both datasets are manually annotated by domain experts to ensure accuracy and

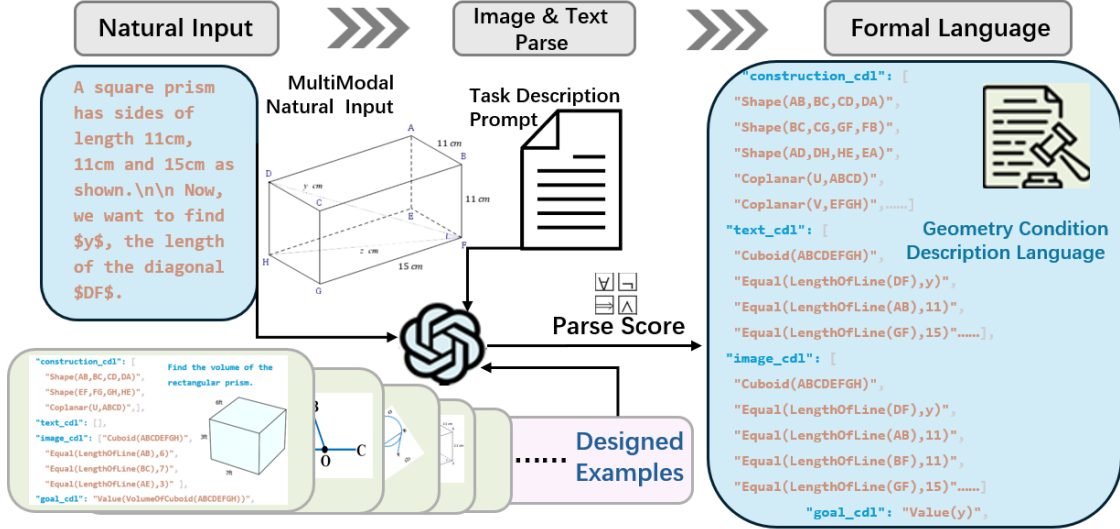


Figure 4. Overall process of parsing images and text into geometry condition description language (CDL)

consistency, covering complementary geometric scenarios (solid and plane) and providing a comprehensive basis for parsing tasks.

4.1. Dataset Collection

SolidFGeo2k and PlaneFGeo3k are constructed to focus on geometric problem solving, covering two core domains of geometric reasoning. SolidFGeo2k comprises 1,908 stereometric problems centered on geometric solution derivation, while PlaneFGeo3k consists of 3,022 plane geometric problems. Both datasets adhere to a unified raw content collection framework, capturing three essential components for each problem.

First, problem descriptions are collected as structured natural language text, precisely conveying geometric configurations, given conditions, and solution targets. These descriptions are sourced from other datasets and renowned educational [6] and research resources [31], ensuring alignment with practical geometric reasoning needs and encompassing a variety of distinct problem types [29]. Second, geometric images are paired with each problem description, visually representing the spatial relationships, shape compositions, and key elements of the geometric scenario [39]. Third, standard answers are compiled for each problem, providing numerical results (e.g., volume, area, length, angle) or definitive descriptive conclusions (e.g., spatial relation confirmations) derived from standard geometric solution processes. These answers serve as the ground truth for validating problem-solving correctness. The collection process prioritizes authenticity and diversity, ensuring the raw content reflects real-world geometric problem characteristics. More details are provided in Appendix B.

4.2. Manual Annotation

To transform raw problem content into actionable resources for geometric formalization and model training, datasets undergo systematic manual annotation by experts. All experts have experience in formal mathematical annotation. The annotation work follows standardized protocols and leverages professional tools. Formal language encoding is implemented to translate the annotated information into geometric description language (CDL). This encoding unifies text and image semantics into a standardized structured format. The encoding process adheres to strict syntax rules to maintain consistency across the dataset. To ensure annotation quality, a two-stage validation mechanism is adopted: 20% of entries are randomly selected for cross-validation by an independent expert team, and inter-annotator agreement is measured using Cohen’s Kappa [9]. SolidFGeo2k achieves a Kappa score of 0.89, while PlaneFGeo3k reaches 0.91—both indicating “almost perfect” consistency. Final adjustments are made to resolve discrepancies, ensuring the annotations meet high standards of accuracy and reliability for downstream geometric reasoning tasks.

5. Parse2Reasoning Method

5.1. MultiModal Formalization Parser (M2FP)

The translation of natural language geometric descriptions into formal languages is a foundational step in enabling automated geometric reasoning, as structured formalizations allow for precise computation of spatial relationships, property deductions, and theorem verification. This process involves two core stages: parsing (the autoformalization process of converting natural language to formal language) and reasoning (leveraging formal language for inference). To

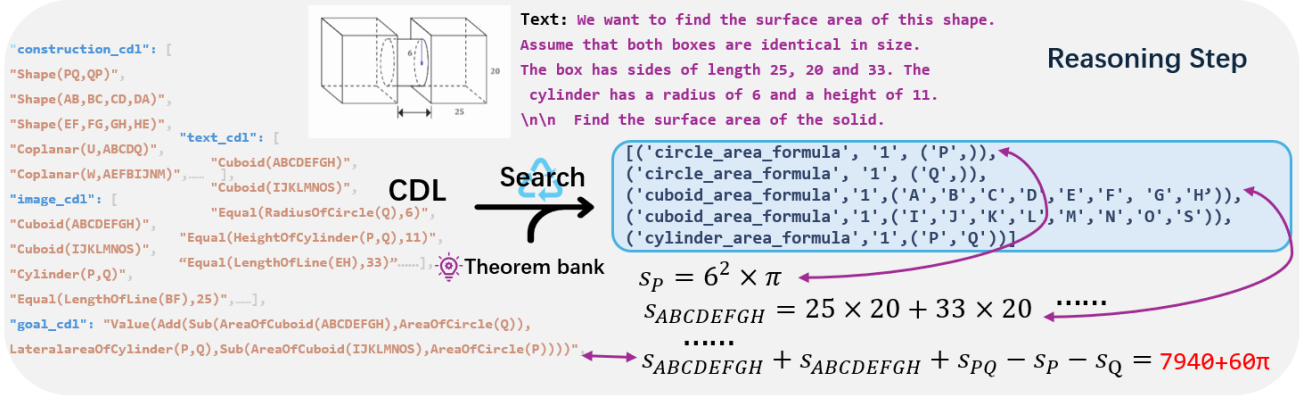


Figure 5. Reasoning using geometric condition description language (CDL)

ensure robustness, both stages require rigorous evaluation, with parsing quality directly impacting downstream reasoning performance. Below, we outline the pipeline structure, evaluation methods, and experimental design to assess this workflow. More details in Appendix C.1.

As shown in Fig. 4, this process starts with a targeted prompt engineering approach: specialized prompts are constructed using expertly designed example sets that cover all basic predicates. These examples can express predicates and formal language without involving complex geometric relationships, and each includes geometric descriptions and their corresponding formalizations. The model is guided to parse unseen geometric content into formal language using known predicates and formalized language, with these examples serving as structural and logical references. These examples will be presented to MLLMs along with a task description prompt of several hundred words to obtain the formal language (i.e., Condition Description Language).

5.2. Solid Geometry Reasoning Engine (SGRE)

Building on the Multimodal Formalization Parser, we introduce the Solid Geometry Reasoning Engine (SGRE), which is a dedicated module that drives inference using a comprehensive library of solid geometry predicates and theorems. SGRE focuses on transforming parsed CDL representations into actionable solutions through rigorous symbolic deduction, addressing the core challenge of multi-step geometric reasoning. Theoretically, provided that the problem itself is valid and the upstream parsing is accurate, a sound search mechanism will invariably yield a correct and verifiable solution process (See Fig. 5).

Starting from the CDL output of the parser, SGRE initializes a node-based reasoning tree. (See Algorithm 1) Each node represents a geometric state: expandable nodes correspond to unresolved sub-problems, solved nodes mark completed sub-goals, and failed nodes indicate invalid theorem applications. The engine iteratively matches expandable

Algorithm 1 Theorems Search and Verification

Require: *tree*: a tree with the known problem conditions as the node.

Ensure: *theorem_seqs*: list of theorem sequence for solving.

Initialize a list *theorem_seqs*

$node \leftarrow tree.get_expandable()$

while *node* is not None **do**

$solved \leftarrow node.apply_theorem()$

if *solved* **then**

$node.state \leftarrow SOLVED$

$theorem_seqs \leftarrow node.get_theorem_seqs()$

break

end if

$node.state \leftarrow EXPANDED$

$l \leftarrow node.expand()$

if $l = 0$ **then**

$node.state \leftarrow UNSOLVED$

end if

$node \leftarrow tree.get_expandable()$

end while

nodes against applicable theorems from the library, applying logical substitutions and calculations to generate new states, and computes the final result through chained deduction.

Since SGRE addresses a NP problem, most failed cases arise from combinatorial explosion, which prevents finding a goal-satisfying solution within a reasonable time. Notably, over 80% of solvable problems can be resolved within 1.2 seconds and 57 reasoning steps. The majority of unsolved cases stem from erroneous CDL outputs or inherent flaws in the problem itself, thereby enabling SGRE to also assess the validity of problem premises and solutions.

By evaluation on the SolidFGeo2k dataset, SGRE achieves an 78% accuracy rate across complex tasks, val-

idating the effectiveness of its predicate-theorem framework. By grounding inference entirely in structured solid geometric knowledge, SGRE ensures traceable, human-aligned reasoning, complementing the parser’s role in converting multimodal inputs to formal representations. Together, these components form a complete pipeline for automated solid geometry problem-solving. More details are in Appendix D.

6. Experiments

To validate the efficacy of the Hilbert-Geo framework in facilitating solid geometry reasoning and quantify its superior performance compared to state-of-the-art multimodal large language models (MLLMs), we have devised a suite of comprehensive experiments. In this section, we first elaborate on the experimental design and setup, followed by a detailed presentation of the quantitative results pertaining to both the parsing phase and the reasoning phase. Subsequently, we conducted an in-depth analysis of the empirical findings to elucidate the underlying mechanisms and practical implications. More details are provided in Appendix E.

6.1. Experimental Setting

Parsing step. As shown in Fig. 4, the parsing step, as the core perceptual component of the Hilbert-Geo framework, is subjected to independent performance evaluation to decouple its intrinsic effectiveness from the interference of the subsequent reasoning step. To ensure the comprehensiveness and representativeness of the evaluation, we conducted systematic testing in five closed-source models and four open-source models, with four gradient sample quantities (15, 25, 35, and 45 samples respectively). In the parsing steps of Section 5.1, these samples were sampled from expertly designed example sets that cover diverse task scenarios and data distributions.

Reasoning step. To comprehensively assess the performance of the Hilbert-Geo framework, we conduct five rounds of evaluations on a diverse set of multimodal large language models (MLLMs) across the benchmark datasets SolidFGeo2k, PlaneFGeo3k, and Mathverse-Solid. This evaluation covers 5 open-source and 4 closed-source models, ensuring a thorough comparison across different model types and access paradigms.

To establish a human performance baseline, we recruited 50 high school students to independently complete the closed-book questions. Furthermore, we feed the parsing results derived from Section 5.2 into the Solid Geometry Reasoning Engine, which characterize the models’ perceptual ability to convert geometric inputs into formal CDL. Here, we assess the success rate of geometric reasoning, measuring how effectively each model executes deductive processes based on the parsed formal structures.

6.2. Experimental Results

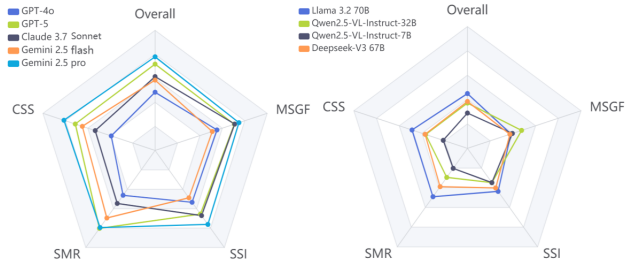


Figure 6. Performances for Different Subjects (CSS, SMR, SSI, MSGF, See Table 1) based on Hilbert-Geo

Table 1. MLLMs and Hilbert-Geo (Gemini-2.5-pro 45 samples) performances on SolidFGeo2k; Four fine grains: Composite Solid Structures (CSS), Spatial Metric Relations (SMR), Solid Shape Identification (SSI), Measurement of Solid Geometric Forms (MSGF); The underline represents the best performance of MLLMs

| Model | Overall.Avg | CSS | SMR | SSI | MSGF |
|-------------------------------------|-------------|-------------|-------------|-------------|-------------|
| Closed-source MLLMs | | | | | |
| GPT-4o[26] | 35.8 | 25.9 | 27.8 | 39.2 | 40.0 |
| GPT-5[28] | 50.6 | 51.2 | 55.4 | 40.6 | 46.8 |
| Claude 3.7 Sonnet[1] | 47.1 | 39.2 | 40.4 | <u>52.9</u> | <u>56.8</u> |
| Gemini 2.5 Flash[11] | 39.8 | 50.7 | 55.4 | 34.6 | 36.8 |
| Gemini 2.5 Pro[11] | <u>54.2</u> | <u>60.2</u> | <u>62.4</u> | 48.2 | 49.8 |
| Open-source MLLMs | | | | | |
| Llama 3.3 70B[21] | 33.6 | 36.3 | 34.4 | 31.1 | 28.7 |
| Qwen2.5-VL-Instruct-32B[4] | 29.8 | 27.2 | 19.9 | 35.2 | 38.1 |
| Qwen2.5-VL-Instruct-7B[4] | 20.2 | 17.7 | 10.7 | 25.2 | 30.1 |
| Deepseek-V3 67B[10] | 30.1 | 11.7 | 11.3 | 28.6 | 27.8 |
| Human Performances | | | | | |
| Human | 81.8 | 84.3 | 81.2 | 86.1 | 78.7 |
| Hilbert-Geo | | | | | |
| Hilbert-Geo (Ground-Truth) (Ours) | 78.7 | 80.5 | 84.1 | 76.3 | 75.1 |
| Hilbert-Geo (Gemini-2.5-Pro) (Ours) | 77.3 | 80.3 | 79.4 | 76.2 | 74.8 |

The findings in Table 1 underscore the inherent challenges of Solid Geometry. Gemini 2.5 Pro emerges as the top-performing model with an overall accuracy of 54.2%, followed by GPT-5 at 50.6% and Claude-3.7-Sonnet at 47.1%. Notably, all other models score below 40%, highlighting the significant hurdles that solid geometry reasoning presents even for cutting-edge large language models.

Across fine-grained tasks that demand robust reasoning, including Composite Solid Structures (CSS), Spatial Metric Relations (SMR), Solid Shape Identification (SSI), and Measurement of Solid Geometric Forms (MSGF), notable performance gaps persist among leading models. Gemini 2.5 Pro takes the lead in SMR with a score of 62.4% but lags behind in SSI, achieving only 48.2%. Open-source models, with Llama 3.3 70B as a representative example (scoring 36.3% in CSS and 28.7% in MSGF), consistently underperform compared to their closed-source counterparts.

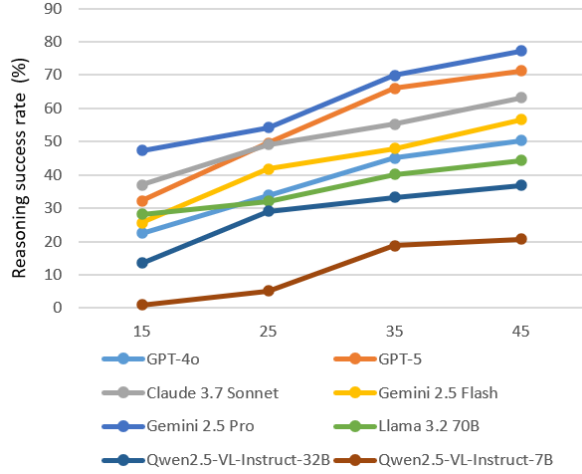


Figure 7. Reasoning performance of MLLMs under different numbers of samples based on Hilbert-Geo

Critically, all these models remain significantly behind human performance, highlighting the current limitations in replicating human-level reasoning in solid geometry tasks. Hilbert-Geo, however, presents a different scenario (See Fig. 6). When evaluated on Hilbert (using 45 samples), Hilbert-Geo achieves the highest performance across all key dimensions: 80.3% in CSS, 79.4% in SMR, 76.2% in SSI, 74.8% in MSGF, and an overall score of 77.3%. It outperforms leading models like Gemini 2.5 Pro and approaches human-level performance.

6.3. Ablation study

6.3.1. Parsing Performance

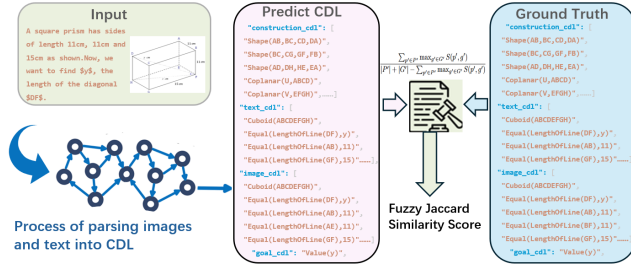


Figure 8. Fuzzy Jaccard Similarity Score between Predicted CDL and Ground Truth

As shown in Fig. 8, for the quantitative assessment of parsing performance, we adopted the Fuzzy Jaccard Similarity as the core accuracy metric. This metric introduces a fuzzy matching mechanism: it first computes the matching scores between the predict CDL results and the ground truth across multiple dimensions, then delineates the fuzzy intersection and fuzzy union based on these continuous matching scores, and finally quantifies the

similarity between the two sets by calculating the ratio of the fuzzy intersection to the fuzzy union:

$$\text{Score} = \frac{\sum_{p' \in P'} \max_{g' \in G'} S(p', g')}{|P'| + |G'| - \sum_{p' \in P'} \max_{g' \in G'} S(p', g')} \quad (1)$$

P' is the normalized predicted CDL set; G' is the normalized ground truth CDL set; $p' \in P'$; $g' \in G'$; $S(p', g')$ is the fuzzy matching scoring function; More details in Appendix C.2.

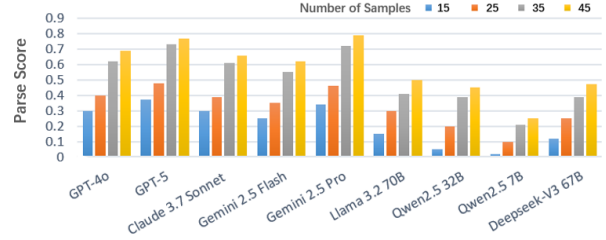


Figure 9. The parsing scores of various MLLMs under different sample quantities (More datasets' results in Appendix C.3.)

As shown in Fig. 9, the experimental results validate that the parsing step of Hilbert-Geo can effectively distinguish the performance of different MLLMs, with GPT-5 and Gemini 2.5 Pro standing out as the most effective models for the parsing phase. Overall, they demonstrate the most robust performance, maintaining a score above 0.7 with 45 samples, which indicates their strong capability in parsing images and text into CDL within the formal framework. This lays a solid foundation for the subsequent reasoning step in the Hilbert-Geo framework, as a high-quality parsing output is crucial for accurate geometry reasoning.

6.3.2. Impact of Various Models and Number of Samples

Table 2. Performance of Different Models on Hilbert-Geo (45 Samples): Accuracy, Average Time per Solved Problem, and Reasoning Steps; The underline represents the best performance of Hilbert-Geo

| Model | Overall Avg | CSS | SMR | SSI | MSGF | Avg.time | Avg.steps |
|---|-------------|-------------|-------------|-------------|-------------|-------------|--------------|
| Closed-source MLLMs | | | | | | | |
| Hilbert-Geo (GPT-4o)[26] | 50.3 | 39.1 | 46.2 | 53.4 | 55.2 | 38.1 | 112.6 |
| Hilbert-Geo (GPT-5)[28] | 71.2 | 71.2 | <u>80.3</u> | 65.5 | 70.7 | 77.5 | 152 |
| Hilbert-Geo (Claude 3.7 Sonnet)[11] | 63.2 | 53.4 | 54.6 | 67.1 | 71.0 | 50.0 | 129.2 |
| Hilbert-Geo (Gemini 2.5 Flash)[11] | 56.5 | 64.9 | 69.6 | 48.8 | 51.0 | 47.1 | 117.9 |
| Hilbert-Geo (Gemini 2.5 Pro)[11] | <u>77.3</u> | <u>80.3</u> | 79.4 | <u>76.2</u> | <u>74.8</u> | <u>81.2</u> | <u>159.1</u> |
| Open-source MLLMs | | | | | | | |
| Hilbert-Geo (Llama 3.3 70B)[21] | 44.3 | 48.8 | 49.1 | 43.7 | 38.3 | 28.0 | 101.1 |
| Hilbert-Geo (Qwen2.5-VL-Instruct-32B)[4] | 36.9 | 36.8 | 29.5 | 34.8 | 47.7 | 14.2 | 76.9 |
| Hilbert-Geo ((Qwen2.5-VL-Instruct-7B)[4]) | 30.7 | 21.3 | 20.3 | 34.8 | 39.6 | 2.9 | 32.0 |
| Hilbert-Geo ((Deepseek-V3 67B)[10]) | 38.8 | 37.3 | 38.9 | 40.2 | 37.4 | 22.9 | 90.3 |
| Formal Language Ground Truth | | | | | | | |
| Hilbert-Geo (CDL) | 78.7 | 80.5 | 84.1 | 76.3 | 75.1 | 88.0 | 174.6 |

As shown in Table 2 and Table 1, it achieves a remarkable qualitative breakthrough in reasoning, boasting an average reasoning accuracy of 77.3% in datasets with a scale 1.5 times that of pure MLLMs (See Fig. 10). Even with the

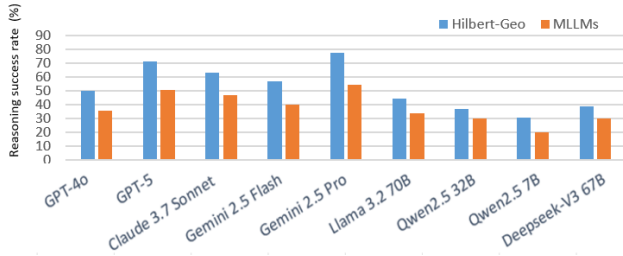


Figure 10. Comparison of Reasoning Performances between Hilbert-Geo (45 samples) and MLLMs

smallest sample size of 15 examples, its accuracy in SolidFGeo2k reaches 42.1% (See Fig. 7), surpassing Deepseek-V3 67B’s peak performance.

Across pivotal benchmarks, Hilbert-Geo attains 77.3% accuracy on SolidFGeo2k and consistently outperforms state-of-the-art MLLMs and specialized solvers. This superiority originates from two core strengths of the Hilbert-Geo framework: firstly, the CDL effectively encapsulates both the intrinsic geometric properties and the problem-specific conditions, while the SGRE conducts rigorous formal reasoning to derive the final solution. This symbol-driven approach ensures the reasoning process is rigorous and logically coherent; Secondly, the framework effectively steers MLLMs’ geometric intuition during the parsing stage, guaranteeing that initial geometric conditions are unambiguous, precise, and devoid of hallucinations.

Additionally, from Fig. 7, we can observe that models with better performance have longer inference times and more steps. This is because the CDL complexity after parsing difficult questions is high, while the search in the inference process is fixed (always exponential complexity). Therefore, the average time and the average steps also indirectly indicate the parsing ability of the model.

6.3.3. Error Analysis



Figure 11. Error distribution of Hilbert-Geo (Gemini 2.5 pro and GPT-5 with 45 samples)

As illustrated in Fig. 11, the errors occurring in Hilbert-Geo primarily stem from three key sources: CDL distortion during the parsing phase, combinatorial explosion induced by excessively complex problem combinations in the reasoning phase, and inherent defects in the problem condi-

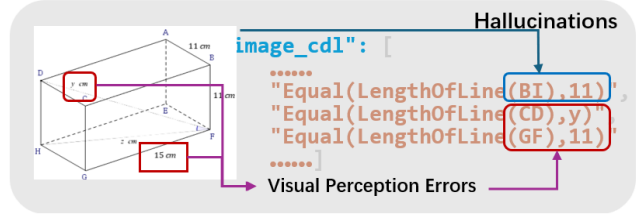


Figure 12. example of hallucination and Visual Perception Error

tions themselves. For CDL distortion in the parsing phase, we performed two targeted analyses on CDL, focusing on hallucinations and Visual Perception Errors (See Fig. 12). The results indicated a substantial reduction in both the incidence of hallucinations and Visual Perception Errors, which fully demonstrates that the parsing phase of Hilbert-Geo can effectively alleviate these two types of issues. In terms of the reasoning phase, we adjusted the time limit setting by removing the original 300-second constraint, we tested 103 problems that were prone to timeouts under the former setting; 87% of these problems were successfully solved within the tested time frame, offering support for the completeness of Hilbert-Geo’s knowledge base. Theoretically, Hilbert-Geo exhibits no calculation and reasoning errors throughout the reasoning process.

7. Conclusion

In this paper, we introduce Hilbert-Geo, the first unified solid geometric formal framework to tackle the unique challenges of automated solid geometric reasoning, aiming to address a long-standing gap in AI systems’ ability to handle spatial logic and multimodal 3D diagram interpretation. By integrating a multimodal formalization parser and a solid geometry reasoning engine, which are tailored to capture 3D entity relationships and mitigate spatial hallucinations common in MLLMs, the framework fills this critical gap. Extensive experiments conducted on our curated SolidFGeo2k, PlaneFGeo3k, and MathVerse-solid datasets validate that Hilbert-Geo outperforms leading MLLMs, as it can effectively alleviate reasoning hallucinations, ensure logical consistency, and guide geometric intuition through formalized representations. Additionally, the framework targets the limited capability of existing methods in addressing vector-related tasks and problems requiring sophisticated auxiliary line constructions, as these gaps further underscore the need for a specialized approach. Furthermore, error analysis reveals that visual perception and logical reasoning deficits are the primary bottlenecks for current MLLMs in solid geometry, which highlights the value of Hilbert-Geo’s structured approach in mitigating these limitations.

Acknowledgments

This work was supported by National Natural Science Foundation of China under No.62436009, and Jiangsu Science and Technology Programme BK20251812, and Open Research Fund of The State Key Laboratory of Multimodal Artificial Intelligence Systems.

References

- [1] Anthropic. Claude 3.7 sonnet system card. <https://www.anthropic.com/claude-3-7-sonnet-system-card>, 2025. System card for Claude 3.7 Sonnet.
- [2] Dennis S. Arnon, George E. Collins, and Scott McCallum. Cylindrical algebraic decomposition i: The basic algorithm. *SIAM Journal on Computing*, 13(4):865–877, 1984.
- [3] Lucian Bădescu. *Projective Geometry and Formal Geometry*. Birkhäuser Basel, 2004.
- [4] Shuai Bai, Keqin Chen, Xuejing Liu, et al. Qwen2.5-VL technical report. *arXiv preprint arXiv:2502.13923*, 2025.
- [5] Peter W. Battaglia, Jessica B. Hamrick, Victor Bapst, et al. Relational inductive biases, deep learning, and graph networks. *arXiv preprint arXiv:1806.01261*, 2018.
- [6] Jiaqi Chen, Jianheng Tang, Jinghui Qin, Xiaodan Liang, Lingbo Liu, Eric P. Xing, and Liang Lin. GeoQA: A geometric question answering benchmark towards multimodal numerical reasoning. In *Findings of the Association for Computational Linguistics: ACL-IJCNLP 2021*, pages 513–523, 2021.
- [7] Jiaqi Chen, Tong Li, Jinghui Qin, et al. UniGeo: Unifying geometry logical reasoning via reformulating mathematical expression. In *Proceedings of the 2022 Conference on Empirical Methods in Natural Language Processing*, pages 3313–3323, 2022.
- [8] Xingyu Chen, Jiahao Xu, Tian Liang, et al. Do NOT think that much for $2+3=?$ on the overthinking of long reasoning models. In *Proceedings of the 42nd International Conference on Machine Learning*, pages 9487–9499. PMLR, 2025.
- [9] Jacob Cohen. A coefficient of agreement for nominal scales. *Educational and Psychological Measurement*, 20(1):37–46, 1960.
- [10] DeepSeek-AI. DeepSeek-V3 technical report. *arXiv preprint arXiv:2412.19437*, 2024.
- [11] Google. Gemini 2.5: Updates to our family of thinking models. <https://developers.googleblog.com/en/gemini-2-5-thinking-model-updates/>, 2025. Introduces Gemini 2.5 Pro and Gemini 2.5 Flash updates.
- [12] Muhammad Usman Hadi, Qasem Al Tashi, Abbas Shah, et al. Large language models: A comprehensive survey of its applications, challenges, limitations, and future prospects. *TechRxiv*, 2024. Preprint, version 6.
- [13] Osman Hasan and Sofiene Tahar. Formal verification methods. In *Encyclopedia of Information Science and Technology, Third Edition*, pages 7162–7170. IGI Global Scientific Publishing, 2015.
- [14] Takayuki Hibi, editor. *Gröbner Bases: Statistics and Software Systems*. Springer Tokyo, 2014. Copyright 2013.
- [15] Pengpeng Jian, Fucheng Guo, Yanli Wang, et al. Solving geometry problems via feature learning and contrastive learning of multimodal data. *Computer Modeling in Engineering & Sciences*, 136(2):1707–1728, 2023.
- [16] Juyong Jiang, Fan Wang, Jiasi Shen, et al. A survey on large language models for code generation. *ACM Transactions on Software Engineering and Methodology*, 35(2):1–72, 2026.
- [17] Chaoyu Li, Eun Woo Im, Pooyan Fazli, et al. Vidhalluc: Evaluating temporal hallucinations in multimodal large language models for video understanding. In *Proceedings of the IEEE/CVF Conference on Computer Vision and Pattern Recognition (CVPR)*, pages 13723–13733, 2025.
- [18] Zhaoyu Li, Jialiang Sun, Logan Murphy, et al. A survey on deep learning for theorem proving. In *Proceedings of the First Conference on Language Modeling*, 2024.
- [19] Pan Lu, Ran Gong, Shibiao Jiang, et al. Inter-GPS: Interpretable geometry problem solving with formal language and symbolic reasoning. In *Proceedings of the 59th Annual Meeting of the Association for Computational Linguistics and the 11th International Joint Conference on Natural Language Processing (Volume 1: Long Papers)*, pages 6774–6786, Online, 2021. Association for Computational Linguistics.
- [20] Pan Lu, Hritik Bansal, Tony Xia, et al. MathVista: Evaluating mathematical reasoning of foundation models in visual contexts. In *The Twelfth International Conference on Learning Representations*, 2024. Oral presentation.
- [21] Meta. Llama 3.3 model cards and prompt formats, 2024. Official Meta documentation for Llama 3.3, release date: December 6, 2024.
- [22] Logan Murphy, Kaiyu Yang, Jialiang Sun, et al. Autoformalizing euclidean geometry. In *Proceedings of the 41st International Conference on Machine Learning*, pages 36847–36893. PMLR, 2024.
- [23] Humza Naveed, Asad Ullah Khan, Shi Qiu, et al. A comprehensive overview of large language models. *ACM Transactions on Intelligent Systems and Technology*, 16(5):1–72, 2025.
- [24] Maizhen Ning, Qiu-Feng Wang, Kaizhu Huang, and Xiaowei Huang. A symbolic characters aware model for solving geometry problems. In *Proceedings of the 31st ACM International Conference on Multimedia (MM '23)*, pages 7767–7775, New York, NY, USA, 2023. ACM.
- [25] Maizhen Ning, Zihao Zhou, Qiufeng Wang, Xiaowei Huang, and Kaizhu Huang. GNS: Solving plane geometry problems by neural-symbolic reasoning with multi-modal llms. In *Proceedings of the AAI Conference on Artificial Intelligence*, pages 24957–24965, 2025.
- [26] OpenAI. Hello gpt-4o. <https://openai.com/index/hello-gpt-4o/>, 2024. OpenAI announcement.
- [27] OpenAI. Introducing gpt-5. <https://openai.com/index/introducing-gpt-5/>, 2025. OpenAI announcement.
- [28] OpenAI. GPT-5 system card. <https://openai.com/index/gpt-5-system-card/>, 2025. OpenAI system card.

- [29] M. Pittalis and C. Christou. Types of reasoning in 3d geometry thinking and their relation with spatial ability. *Educational Studies in Mathematics*, 75(2):191–212, 2010.
- [30] Gemini Team. Gemini: A family of highly capable multi-modal models. *arXiv preprint arXiv:2312.11805*, 2023.
- [31] Ke Wang, Junting Pan, Weikang Shi, et al. Measuring multi-modal mathematical reasoning with math-vision dataset. In *NeurIPS 2024 Datasets and Benchmarks Track*, 2024.
- [32] Peijie Wang, Chao Yang, Zhong-Zhi Li, et al. SolidGeo: Measuring multimodal spatial math reasoning in solid geometry. In *NeurIPS 2025 Datasets and Benchmarks Track*, 2025. Poster.
- [33] Yue Wang, Qiuzhi Liu, Jiahao Xu, Tian Liang, Xingyu Chen, Zhiwei He, Linfeng Song, Dian Yu, Juntao Li, Zhuosheng Zhang, et al. Thoughts are all over the place: On the underthinking of o1-like llms. *arXiv preprint arXiv:2501.18585*, 2025.
- [34] Likang Wu, Zhi Zheng, Zhaopeng Qiu, et al. A survey on large language models for recommendation. *World Wide Web*, 27(5):60, 2024.
- [35] Weiming Wu, Jiachen Ye, Zihao Wang, Ziyi Zhou, Yifan Li, and Luzhen Guo. Nesygeo: A neuro-symbolic framework for multimodal geometric reasoning data generation. *arXiv preprint arXiv:2505.17121*, 2025.
- [36] Renqiu Xia, Mingsheng Li, Hancheng Ye, et al. GeoX: Geometric problem solving through unified formalized vision-language pre-training. In *The Thirteenth International Conference on Learning Representations*, 2025.
- [37] Renrui Zhang, Dongzhi Jiang, Yichi Zhang, et al. MathVerse: Does your multi-modal llm truly see the diagrams in visual math problems? In *European Conference on Computer Vision*, pages 169–186. Springer, 2024.
- [38] Xiaokai Zhang, Na Zhu, Yiming He, et al. FormalGeo: An extensible formalized framework for olympiad geometric problem solving. *arXiv preprint arXiv:2310.18021*, 2023.
- [39] Junbo Zhao, Ting Zhang, Jiayu Sun, Mi Tian, and Hua Huang. Pi-GPS: Enhancing geometry problem solving by unleashing the power of diagrammatic information. In *Proceedings of the IEEE/CVF International Conference on Computer Vision (ICCV)*, pages 1526–1536, 2025.
- [40] Wayne Xin Zhao, Kun Zhou, Junyi Li, et al. A survey of large language models. *arXiv preprint arXiv:2303.18223*, 2023.

Hilbert-Geo: Solving Solid Geometric Problems by Neural-Symbolic Reasoning

Supplementary Material

A. Solid Geometry Formal Language

A.1. Formal Geometry Representation

In the domain of solid geometry, simple geometric bodies serve as fundamental units that are combined into complex geometries via combinatorial strategies. This section provides a formal proof that the solid construction operation constitutes a commutative semigroup.

Previous work on Geometry Formalization Theory has shown that the formal representation of plane geometry is a semigroup (Section. 3.1). In solid geometry, we elevate this representation to a set of faces. The plane geometric category is encapsulated as an entity, which serves as the foundational reference for constructing solid geometric models.

Let the formal representation of a simple polyhedron \mathcal{P} be a set R_P (Here, the polyhedron refers to a figure that is topologically homeomorphic to a \mathbb{R}^3 sphere):

$$R_P = \{f_1^{(P)}, f_2^{(P)}, \dots, f_m^{(P)}\} \quad (2)$$

where each face $f_i^{(P)}$ is an ordered list of vertices (following the right-hand rule with outward normal vectors) describing the boundary of that face:

$$f_i^{(P)} = (v_1, v_2, \dots, v_k) \quad (3)$$

Definition of Composition Operation (\oplus_{3D}): This is the foundation of the combined strategy, let polyhedra A and B be joined via a shared interface. Let S_A denote the shared face in A , and S_B denote the corresponding shared face in B (note: geometrically, the vertex order of S_A is the reverse of S_B). The solid composition operation is defined as the set union minus the symmetric intersection (the internal contact faces), as shown in Eq. 4:

$$R_A \oplus_{3D} R_B = (R_A \setminus \{S_A\}) \cup (R_B \setminus \{S_B\}) \quad (4)$$

Theorem A.1. *The formal representation of solid geometry is closed under the operation \oplus_{3D} .*

Proof. By definition, a valid object in the solid formal system is a "set of faces bounding a closed 3D space".

1. Let R_A and R_B be face sets of two valid polyhedra.
2. Execute the operation $R_{result} = R_A \oplus_{3D} R_B$.
3. This operation removes the internal contact faces (S_A and S_B) and retains all external surfaces.
4. According to the generalization of Euler's formula for manifolds, when two closed manifolds are glued along a simply connected face and that face is removed, the remaining surface still constitutes a closed 2-manifold (i.e., the boundary of the new polyhedron).

5. Therefore, R_{result} remains a set of faces describing a closed solid.

$$\forall R_A, R_B \in \mathbb{S}, \quad (R_A \oplus_{3D} R_B) \in \mathbb{S} \quad (5)$$

□

Theorem A.2. $R_A \oplus_{3D} R_B = R_B \oplus_{3D} R_A$.

Proof. Let R_A contain m faces and R_B contain n faces. Based on Eq. 4:

$$R_A \oplus_{3D} R_B = \{f \mid f \in R_A \cup R_B, f \neq S_A, f \neq S_B\} \quad (6)$$

Now consider the reverse operation $R_B \oplus_{3D} R_A$:

$$R_B \oplus_{3D} R_A = (R_B \setminus \{S_B\}) \cup (R_A \setminus \{S_A\}) \quad (7)$$

According to set algebra, the union operation is commutative, i.e., $X \cup Y = Y \cup X$. Therefore:

$$(R_A \setminus \{S_A\}) \cup (R_B \setminus \{S_B\}) = (R_B \setminus \{S_B\}) \cup (R_A \setminus \{S_A\}) \quad (8)$$

Substituting back into Eq. 6 and Eq. 7, we obtain:

$$R_A \oplus_{3D} R_B = R_B \oplus_{3D} R_A \quad (9)$$

This indicates that the construction of solid figures is independent of the input order of components. □

Theorem A.3. $(R_A \oplus_{3D} R_B) \oplus_{3D} R_C = R_A \oplus_{3D} (R_B \oplus_{3D} R_C)$.

Proof. setup:

1. Polyhedra A and B share interface faces (S_{AB}, S_{BA}).
2. Polyhedra B and C share interface faces (S_{BC}, S_{CB}).
3. R_A, R_B, R_C are their respective face sets.

Left Hand Side: Let $R_{AB} = R_A \oplus_{3D} R_B$.

$$R_{AB} = (R_A \cup R_B) \setminus \{S_{AB}, S_{BA}\} \quad (10)$$

Next, calculate $R_{AB} \oplus_{3D} R_C$. The contact interface involves B and C (i.e., S_{BC} and S_{CB}):

$$(R_A \oplus_{3D} R_B) \oplus_{3D} R_C = (R_{AB} \cup R_C) \setminus \{S_{BC}, S_{CB}\} \quad (11)$$

$$= ((R_A \cup R_B) \setminus \{S_{AB}, S_{BA}\} \cup R_C) \setminus \{S_{BC}, S_{CB}\} \quad (12)$$

Since S_{AB}, S_{BA} exist only between A and B and do not affect C , the formula simplifies to the total union minus all interface faces:

$$= (R_A \cup R_B \cup R_C) \setminus \{S_{AB}, S_{BA}, S_{BC}, S_{CB}\} \quad (13)$$

Right Hand Side: Let $R_{BC} = R_B \oplus_{3D} R_C$.

$$R_{BC} = (R_B \cup R_C) \setminus \{S_{BC}, S_{CB}\} \quad (14)$$

Next, calculate $R_A \oplus_{3D} R_{BC}$. The contact interface involves A and B :

$$\begin{aligned} R_A \oplus_{3D} (R_B \oplus_{3D} R_C) &= (R_A \cup R_{BC}) \setminus \{S_{AB}, S_{BA}\} \\ &= (R_A \cup ((R_B \cup R_C) \setminus \{S_{BC}, S_{CB}\})) \setminus \{S_{AB}, S_{BA}\} \end{aligned} \quad (15)$$

Similarly, this simplifies to the total union minus all interface faces:

$$= (R_A \cup R_B \cup R_C) \setminus \{S_{AB}, S_{BA}, S_{BC}, S_{CB}\} \quad (17)$$

Comparing Eq. 13 and Eq. 17, the results are identical:

$$(R_A \oplus_{3D} R_B) \oplus_{3D} R_C = R_A \oplus_{3D} (R_B \oplus_{3D} R_C) \quad (18)$$

□

A.2. Predicate Library and Theorem Bank

A.2.1. Predicate Library

The Solid Predicate Library encompasses 120 predicates, comprising 35 fundamental predicates (Table 3) natively integrated into the solver, along with 20 entity types (Table 4), 35 entity relationships (Table 5), and 30 attribute descriptors (Table 6) defined via a dedicated predicate.

Table 3. fundamental predicates

| id | type | name | examples |
|-------|--------------|-------------|--------------------|
| 1 | Construction | Coplanar | Coplanar(ABCD) |
| 2 | Construction | Cospherical | Cospherical(O,ABC) |
| 3 | Construction | Collinear | Collinear(ABC) |
| 4 | Construction | Cocircular | Cocircular(O,ABC) |
| 5 | BasicEntity | Plane | Plane(U) |
| 6 | BasicEntity | Sphere | Sphere(O) |
| | | | |

Table 4. Entities defined for solid geometry using the predicate

| id | type | examples |
|-------|--------|--------------------------|
| 1 | Entity | Cube(ABCDEFGH) |
| 2 | Entity | Cuboid(ABCDEFGH) |
| 3 | Entity | Cone(O,P) |
| 4 | Entity | Cylinder(P,Q) |
| 5 | Entity | Prism(P,Q) |
| 6 | Entity | TriangularPrism(ABC,DEF) |
| | | |

The detailed statements for defining a predicate is as shown in the Tab. 7, including the predicate name and point variable declaration, validity check declaration, multiple representations, and automatic expansion.

Table 5. Relations defined for solid geometry using the predicate

| id | type | examples |
|-------|----------|--|
| 1 | Relation | ParallelBetweenPlane(U,V) |
| 2 | Relation | PerpendicularBetweenPlane(U,V) |
| 3 | Relation | PerpendicularBetweenLineAndPlane(AB,U) |
| 4 | Relation | IsDiameterOfSphere(AB,O) |
| 5 | Relation | IsTangentOfSphere(PA,O) |
| 6 | Relation | IsCentreOfSphere(P,O) |
| | | |

Table 6. Attributions defined for solid geometry using the predicate

| id | type | examples |
|-------|-------------|----------------------------------|
| 1 | Attribution | HeightOfCone(O,P) |
| 2 | Attribution | HeightOfCylinder(P,Q) |
| 3 | Attribution | HeightOfPrism(P,Q) |
| 4 | Attribution | HeightOfTriangularPrism(ABC,DEF) |
| 5 | Attribution | RadiusOfSphere(O) |
| 6 | Attribution | DiameterOfSphere(O) |
| | | |

A.2.2. Theorem Bank

As shown in Table 8, this section presents some representative theorems from the theorem library, demonstrating the formal representation of geometric knowledge used in the automated reasoning system.

These theorems focus on line-plane relationships and solid geometry: plane-to-plane relationships (transitivity), line-to-plane relationships (perpendicular and parallel judgments), sphere formulas (area and volume), and cylinder properties (volume and height judgments). The theorem library contains over 200 such theorems covering comprehensive geometric knowledge from basic properties to advanced relationships.

Table 7. example for defining a predicate

| name | item | content |
|------------------------|--------|--|
| IsMidpointOfLine(M,AB) | | Point(M) |
| | check | Line(AB) |
| | | Collinear(AMB) |
| | multi | M,BA |
| | extend | Equal(LengthOfLine(AM),LengthOfLine(MB)) |

Table 8. Examples from the theorem library.

| theorem | premise | conclusion |
|--|---|--|
| transitivity_between_plane_and_plane | ParallelBetweenPlane(U,V) & ParallelBetweenPlane(V,W) | ParallelBetweenPlane(U,W) |
| perpendicular_judgment_between_line_and_plane | PerpendicularBetweenLine(AD,BD) & PerpendicularBetweenLine(AD,CD) & Coplanar(U,BCD) & ~Coplanar(U,AD) | PerpendicularBetweenLineAndPlane(AD,U) |
| perpendicular_judgment_between_plane_and_plane | PerpendicularBetweenLineAndPlane(AB,U) & Coplanar(V,AB) | PerpendicularBetweenPlane(U,V) |
| parallel_judgment_between_line_and_plane | ParallelBetweenLine(AB,CD) & Coplanar(U,CD) & ~Coplanar(U,AB) | ParallelBetweenLineAndPlane(AB,U) |
| sphere_area_formula | Sphere(O) | Equal(AreaOfSphere(O),Mul(4,pi,RadiusOfSphere(O), RadiusOfSphere(O))) |
| sphere_volume_formula | Sphere(O) | Equal(VolumeOfSphere(O),Mul(4/3,pi, RadiusOfSphere(O),RadiusOfSphere(O), RadiusOfSphere(O))) |
| cylinder_volume_formula_common | Cylinder(P,Q) | Equal(VolumeOfCylinder(P,Q),Mul(AreaOfCircle(P), HeightOfCylinder(P,Q))) |
| height_of_cylinder_judgment | Cylinder(P,Q) & Coplanar(P,A) & Coplanar(Q,B) & PerpendicularBetweenLineAndPlane(AB,P) | Equal(LengthOfLine(AB),HeightOfCylinder(P,Q)) |
| | | |

B. Dataset

B.1. Data and Annotation

SolidFGeo2k (Fig. 13) presents examples of geometric problems under this benchmark, covering various scenarios and tasks related to solid geometry; PlaneFGeo3k (Fig. 14) focuses on the field of plane geometry; MathVerse-solid (Fig. 15) is a representative resource among existing geometric benchmarks, providing abundant supplementary data support for solid geometry tasks. Together, the three constitute a multi-scenario and multi-level dataset system for geometric tasks.

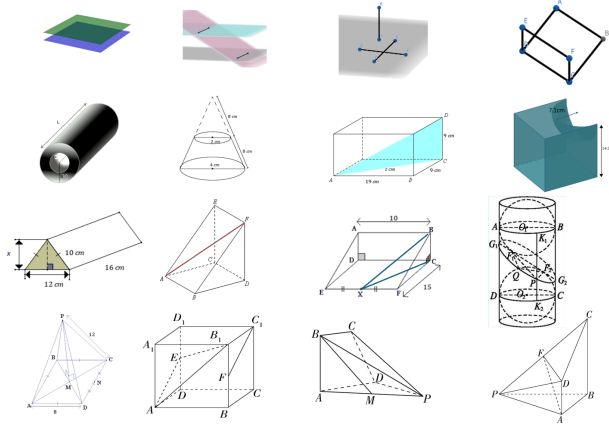


Figure 13. Examples from SolidFGeo2K

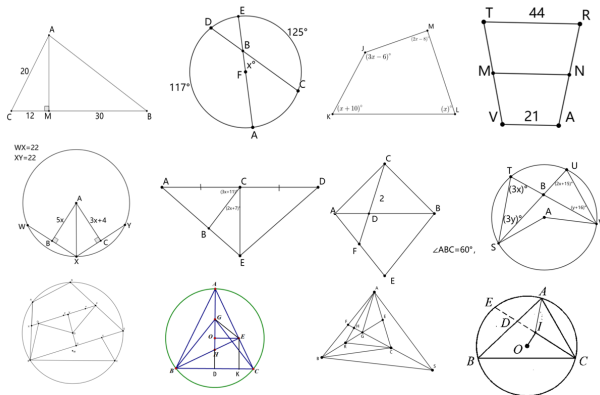


Figure 14. Examples from PlaneFGeo3k

To convert raw problem content into actionable resources for geometric formalization and model training, datasets are systematically annotated manually by experts. This annotation work adheres to standardized protocols and uses professional tools. Meanwhile, formal language encoding is adopted to convert the annotated information into Geometric Description Language. As shown in Figure 16, the geometric description language and the standard answers

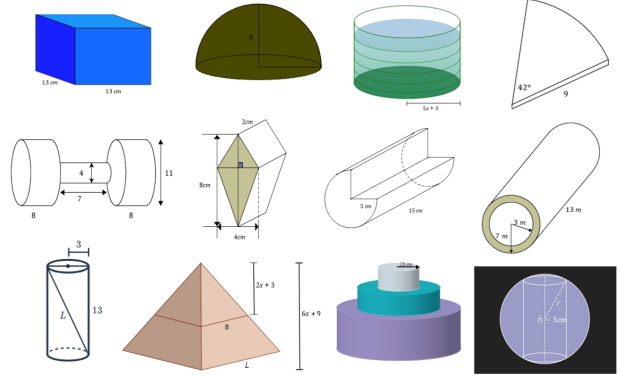


Figure 15. Examples from Mathverse-solid

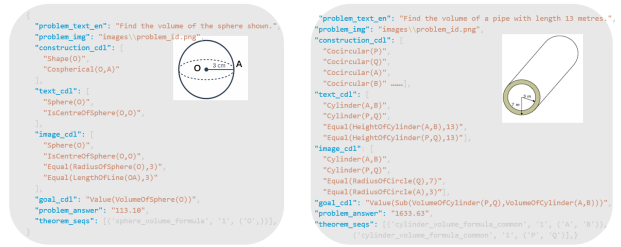


Figure 16. Data Samples from Mathverse-solid and SolidFGeo2k

are annotated based on the original text and images, which serve as the ground truth.

B.2. Data Construction

In our dataset SolidFGeo2k, we collect solid geometric problems in existing datasets except SolidGeo (containing other datasets) as shown in Fig 17. In addition, we add new samples (31.1%) for the comprehensive evaluation. For each problem, we ask **two undergraduat students** to give detailed annotations including parsing results, reasoning process, and correct answer. For your reference, we show differenes to existing datasets in Fig 17.

| Attribute | MathVision | CMMath | DynaMath | MathVerse | OlympiadBench | GeoEval | MVMath | SolidGeo | SolidFGeo2k (ours) |
|--------------------|------------|-----------------|---------------|-----------|---------------|-------------|---------------|------------|--------------------|
| Size | 203 | 122 | 118 | 296 | 448 | 63 | 59 | 2200 | 1908 |
| Fine-grained Label | Subject | Knowledge Point | Question Type | Info Type | Task Type | Eval Subset | Question Type | Sub-domain | Sub-domain |
| Parsing Annotation | X | X | X | X | X | X | X | X | ✓ |
| Reasoning Process | ✓ | ✓ | X | X | X | X | X | X | ✓ |
| LLM Generation | ✓ | ✓ | X | X | X | ✓ | X | ✓ | X |

Figure 17. Comparison of Datasets for Solid Geometry Problems

B.3. Fine-grained Subject categorization

The SolidFGeo2k and Mathverse-solid dataset incorporates fine-grained subject categorization, covering the full spectrum of spatial reasoning skills required. Figure 18 categorizes SolidFGeo2k's content into themes: Composite Solid Structure, Spatial Metric Relations, Solid Shape Identification, and Measurement of Solid Geometric Forms, demon-

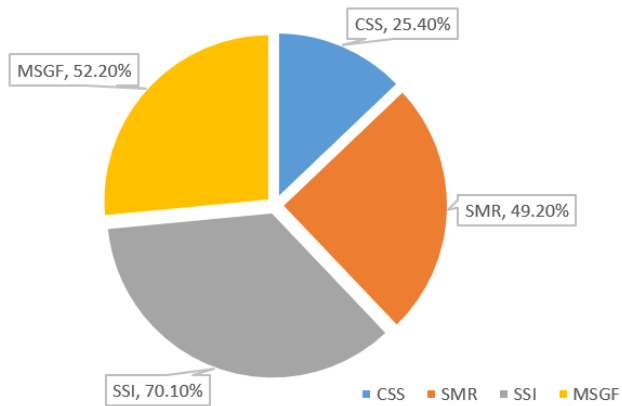


Figure 18. Proportion of different subjects in SolidFGeo2k, note that a single question may match multiple different subjects (Fig. 19)

strating the dataset’s coverage of core solid geometry topics. Figure 18’s pie chart quantifies the proportion of different subjects in SolidFGeo2k: SSI (Solid Shape Identification) accounts for 70.10%, SMR (Spatial Metric Relations) for 49.20%, CSS (Composite Solid Structure) for 25.40%, and MSGF (Measurement of Solid Geometric Forms) for 52.20%. Note that a single problem may belong to multiple subjects, reflecting the interdisciplinary nature of geometric reasoning tasks.

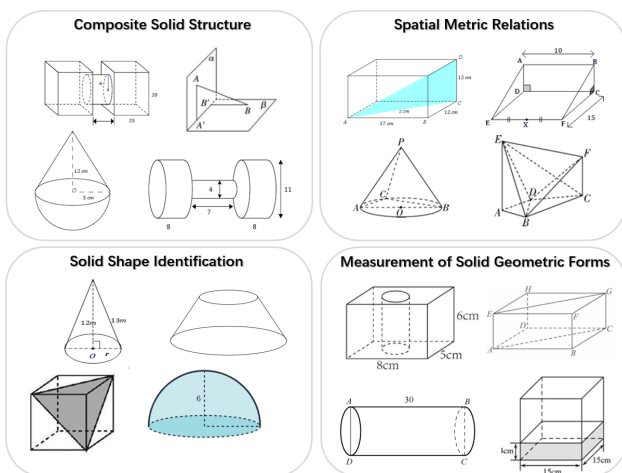


Figure 19. Examples from different subjects

C. Multimodal Formalization Parser (M2FP) Supplementary Information

C.1. M2FP Pipeline Architecture

C.1.1. Overview and Objectives

The Multimodal Formalization Parser (M2FP) translates natural language geometric problem descriptions and visual diagrams into Conditional Description Language (CDL), enabling precise computational reasoning. It integrates information from text and images, converts descriptions into predicate-based CDL format, and ensures completeness and consistency across modalities.

C.1.2. Output Structure

The parser produces a structured CDL representation with four components:

- construction_cdl:** Geometric construction predicates defining fundamental structure (e.g., `Shape(AB,BC,CD,DA)`, `Collinear(PABQ)`, `Cocircular(O)`)
- text_cdl:** Predicates extracted from natural language (e.g., `Equal(LengthOfLine(A,B),5)`, `ParallelBetweenLine(A,B,C,D)`)
- image_cdl:** Predicates derived from visual analysis (e.g., `PerpendicularBetweenLine(AB,BC)`, `Equal(RadiusOfCircle(O),3)`)
- goal_cdl:** A single canonicalized predicate representing the problem’s objective (e.g., `Value(VolumeOfCone(O,P))`)

The system ensures entities in `text_cdl` and `image_cdl` are declared in `construction_cdl`, maintaining cross-modal consistency.

C.1.3. Pipeline Components

Stage 1: Text Parsing The text parsing module extracts entities (points, lines, shapes), maps relations (e.g., “parallel” \rightarrow `ParallelBetweenLine(A,B,C,D)`), parameterizes attributes (e.g., “length of AB is 5” \rightarrow `Equal(LengthOfLine(A,B),5)`), identifies goals (e.g., “Find the volume” \rightarrow `Value(VolumeOfCone(O,P))`), and normalizes the output format.

Stage 2: Image Parsing The image parsing module detects primitives (points, lines, shapes), recognizes visual relations (right-angle marks, parallel indicators, intersections), parses numeric annotations from diagram labels, aligns entities with text mentions, resolves conflicts, and encodes visual information into CDL format consistent with text-derived predicates.

Stage 3: Output Packing The output packing stage consolidates all information into a JSON structure with four

CDL components. Numeric values are formatted without units (supporting expressions like 36π), entities use uppercase letters, and formatting follows strict rules (no extra spaces). The system validates that all entities are declared in `construction_cdl` and all predicates conform to the official vocabulary.

C.2. Fuzzy Matching Evaluation Metrics

We employ fuzzy set-based metrics to evaluate CDL parsing outputs, allowing partial credit for semantically similar predicates that may differ in variable naming or formatting. This section provides complete definitions enabling full reproducibility of the evaluation metrics.

C.2.1. Element Normalization Process

Before computing similarity scores, all CDL elements must be normalized to eliminate differences caused by variable naming conventions. Given a raw CDL set $P = \{p_1, p_2, \dots, p_n\}$ (predicted) or $G = \{g_1, g_2, \dots, g_m\}$ (ground truth), we apply a normalization function `Normalize(\cdot)` to obtain normalized sets $P' = \{\text{Normalize}(p) \mid p \in P\}$ and $G' = \{\text{Normalize}(g) \mid g \in G\}$.

The normalization process follows these steps:

- Remove whitespace:** Strip all spaces from the element string
- Replace variables:** Replace all variable names (single uppercase letters like A, B, C, O, P, etc.) with the placeholder `_V_`
- Preserve numeric values:** Keep all numeric values unchanged
- Process nested structures:** Recursively apply normalization to nested predicate structures
- Normalize variable-only parameters:** If all parameters are variables, replace with `(_V_)`

Examples:

- `Equal(LengthOfLine(A,B),5)` \rightarrow `Equal(LengthOfLine(_V_),5)`
- `Equal(HeightOfCone(O,P),12)` \rightarrow `Equal(HeightOfCone(_V_),12)`
- `Shape(AB,BC,CD,DA)` \rightarrow `Shape(_V_,_V_,_V_,_V_)`
- `Collinear(PABQ)` \rightarrow `Collinear(_V_)`

The complete normalization algorithm is provided in Algorithm 2.

C.2.2. Fuzzy Matching Score Function

The core fuzzy matching score function $S(p', g') \in [0, 1]$ quantifies the similarity between a normalized predicted element $p' \in P'$ and a normalized ground truth element $g' \in G'$. This function is formally defined as:

$$S(p', g') = \begin{cases} 1.0 & \text{if } p' = g' \text{ (exact match)} \\ 0.8 & \text{if } \text{predicate_name}(p') = \text{predicate_name}(g') \\ & \wedge \text{numbers}(p') \cap \text{numbers}(g') \neq \emptyset \\ 0.5 & \text{if } \text{predicate_name}(p') = \text{predicate_name}(g') \\ & \text{only} \\ 0.3 & \text{if } \text{numbers}(p') \cap \text{numbers}(g') \neq \emptyset \\ & \text{only} \\ 0.0 & \text{otherwise} \end{cases} \quad (19)$$

where:

- $\text{predicate_name}(x)$ extracts the predicate name (the substring before the first parenthesis) from normalized element x
- $\text{numbers}(x)$ extracts all numeric values from normalized element x using regular expressions
- The intersection $\text{numbers}(p') \cap \text{numbers}(g') \neq \emptyset$ means at least one numeric value appears in both elements

Examples:

- $S(\text{Equal}(_V_, 5), \text{Equal}(_V_, 5)) = 1.0$ (exact match)
- $S(\text{Equal}(_V_, 5), \text{Equal}(_V_, 5.0)) = 0.8$ (predicate match + number intersection)
- $S(\text{Equal}(_V_, 5), \text{Equal}(_V_, 3)) = 0.5$ (predicate match only)
- $S(\text{Equal}(_V_, 5), \text{LengthOf}(_V_, 5)) = 0.3$ (number intersection only)
- $S(\text{Equal}(_V_, 5), \text{LengthOf}(_V_, 3)) = 0.0$ (no match)

C.2.3. Fuzzy Jaccard Similarity

Given normalized sets P' and G' (obtained from raw sets P and G via the normalization process in Section C.2.1), and using the scoring function $S(p', g')$ defined in Section C.2.2, the Fuzzy Jaccard Similarity extends the standard Jaccard index by replacing exact set intersection with a fuzzy intersection. The fuzzy Jaccard score is computed as:

$$\text{Score}(P, G) = \frac{\sum_{p' \in P'} \max_{g' \in G'} S(p', g')}{|P'| + |G'| - \sum_{p' \in P'} \max_{g' \in G'} S(p', g')} \quad (20)$$

where:

- The numerator $\sum_{p' \in P'} \max_{g' \in G'} S(p', g')$ represents the **fuzzy intersection**: the sum of best-match scores for each predicted element
- The denominator $|P'| + |G'| - \sum_{p' \in P'} \max_{g' \in G'} S(p', g')$ represents the **fuzzy union**: the sum of set sizes minus the intersection

Algorithm 2 CDL Element Normalization

```

1: function NORMALIZECDLELEMENT(element)
2:    $t \leftarrow \text{strip spaces}(\text{element})$ 
3:   if no parentheses in  $t$  then
4:     if is number( $t$ ) then
5:       return  $t$ 
6:     else
7:       return replace all variables with  $\_V\_$ 
8:     end if
9:   else
10:    Process innermost parentheses recursively
11:     $\text{parts} \leftarrow \text{split by commas within parentheses}$ 
12:    for each  $\text{part}$  in  $\text{parts}$  do
13:      if is number( $\text{part}$ ) then
14:        Keep numerical value
15:      else if contains parentheses then
16:         $\text{part} \leftarrow \text{NORMALIZECDLELEMENT}(\text{part})$ 
17:      else
18:         $\text{part} \leftarrow \_V\_$ 
19:      end if
20:    end for
21:    if all parts are  $\_V\_$  then
22:      return  $(\_V\_)$ 
23:    else
24:      return concatenate processed parts
25:    end if
26:  end if
27: end function

```

- P' and G' are obtained by applying normalization to raw sets P and G as described in Section C.2.1

The complete computation algorithm is provided in Algorithm 3.

C.2.4. Boundary Case Handling

Boundary cases are handled as follows: if both sets are empty, Jaccard = 1.0; if one set is empty, Jaccard = 0.0; division by zero is prevented with explicit checks.

C.2.5. Evaluation Algorithms

The evaluation framework implements three core algorithms: normalization (Algorithm 2), Fuzzy Jaccard calculation (Algorithm 3), and score matrix construction (Algorithm 4).

C.2.6. Computational Efficiency

The algorithm computes a $|P'| \times |G'|$ score matrix with $O(|P'| \cdot |G'|)$ time complexity, providing a balance between matching quality and efficiency.

Algorithm 3 Fuzzy Jaccard Similarity Calculation

```
1: function FUZZYJACCARD( $P, G$ )
2:    $P' \leftarrow \{\text{NORMALIZECDLELEMENT}(p) \mid p \in P\}$ 
3:    $G' \leftarrow \{\text{NORMALIZECDLELEMENT}(g) \mid g \in G\}$ 
4:   if boundary case detected then
5:     return boundary Jaccard value (as described in
      Section C.2.4)
6:   end if
7:    $S \leftarrow \text{BUILDScoreMATRIX}(P', G')$ 
8:    $\text{row\_max}[p'] \leftarrow \max_{g' \in G'} S[p', g']$  for each  $p' \in P'$ 
9:    $\text{intersection} \leftarrow \sum_{p' \in P'} \text{row\_max}[p']$ 
10:   $\text{union} \leftarrow |P'| + |G'| - \text{intersection}$ 
11:   $\text{jaccard} \leftarrow \text{intersection}/\text{union}$ 
12:  return  $\text{jaccard}$ 
13: end function
```

Algorithm 4 Matching Score Matrix Construction

```
1: function BUILDScoreMATRIX( $P', G'$ )
2:   Initialize  $S$  as  $|P'| \times |G'|$  matrix
3:   for each  $p' \in P'$  and each  $g' \in G'$  do
4:     if  $p' = g'$  then
5:        $S[p', g'] \leftarrow 1.0$ 
6:     else
7:        $\text{pred\_name} \leftarrow \text{predicate name}(p')$ 
8:        $\text{gt\_name} \leftarrow \text{predicate name}(g')$ 
9:        $\text{pred\_nums} \leftarrow \text{extract numbers}(p')$ 
10:       $\text{gt\_nums} \leftarrow \text{extract numbers}(g')$ 
11:       $\text{name\_equal} \leftarrow (\text{pred\_name} = \text{gt\_name})$ 
12:       $\text{num\_intersect} \leftarrow \text{intersects}(\text{pred\_nums},$ 
       $\text{gt\_nums})$ 
13:      if  $\text{name\_equal}$  and  $\text{num\_intersect}$  then
14:         $S[p', g'] \leftarrow 0.8$ 
15:      else if  $\text{name\_equal}$  then
16:         $S[p', g'] \leftarrow 0.5$ 
17:      else if  $\text{num\_intersect}$  then
18:         $S[p', g'] \leftarrow 0.3$ 
19:      else
20:         $S[p', g'] \leftarrow 0.0$ 
21:      end if
22:    end if
23:  end for
24:  return  $S$ 
25: end function
```

C.3. Parsing Performance Across Models and Sample Sizes

This section presents comprehensive experimental results evaluating the parsing performance of various Multimodal Large Language Models (MLLMs) under different few-shot sample configurations. The evaluation employs fuzzy

matching metrics as described in Section 6.3.1 to assess the quality of CDL parsing across construction predicates, condition predicates (merged text and image), and goal identification.

C.3.1. Parse Score: Comprehensive Performance Metric

The **Parse Score** serves as a comprehensive performance metric that aggregates the parsing quality across three critical components of geometric problem formalization: **Construction**, **Condition**, and **Goal**. The Parse Score is computed as the expectation (average) of the Jaccard similarity scores across these three components:

$$\text{Parse Score} = \frac{1}{3} \sum_{c \in \mathcal{I}} \text{Jaccard}_c \quad (21)$$

where Jaccard_c denotes the Jaccard similarity score for component c , $\mathcal{I} = \{\text{Construction, Condition, Goal}\}$

C.3.2. Component-wise Parsing Performance

To provide detailed insights into the parsing performance, we examine each component individually. The following figures present the Jaccard similarity scores for Construction, Condition, and Goal parsing, respectively, allowing for granular analysis of model strengths and weaknesses across different aspects of geometric formalization.

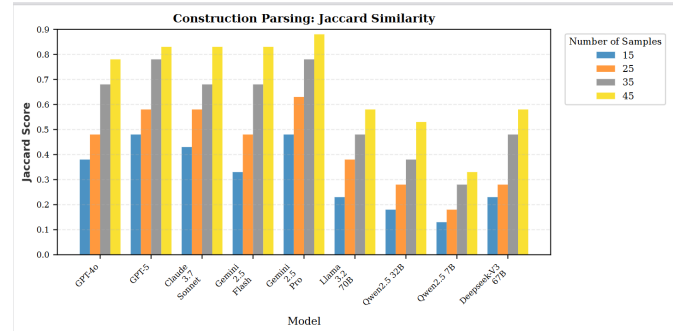


Figure 20. Construction Parsing Performance: Jaccard similarity scores across different models and sample sizes. Construction parsing evaluates the accuracy of extracting geometric structure predicates (e.g., Shape, Collinear, Cocircular). All metrics use fuzzy matching as described in Section 6.3.1.

These three components collectively contribute to the Parse Score, which is computed as their average.

C.3.3. Performance Analysis

The experimental results (Figures 20, 21, and 22) show that Parse Score generally improves as sample size increases from 15 to 45 across all models. Construction parsing achieves the highest scores due to the structured nature of construction predicates, while goal parsing remains the most challenging task. Closed-source models consistently

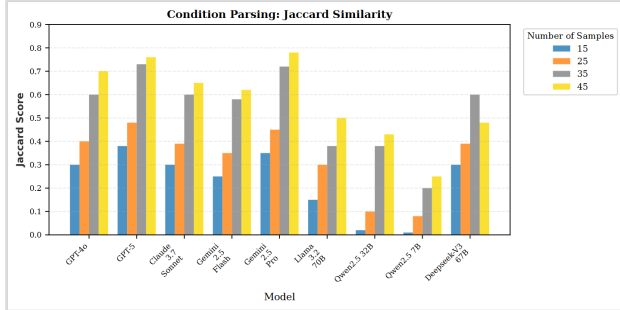


Figure 21. Condition Parsing Performance: Jaccard similarity scores across different models and sample sizes. Condition parsing measures the quality of extracting geometric constraints from problem descriptions and visual diagrams (merged text and image). All metrics use fuzzy matching as described in Section 6.3.1.

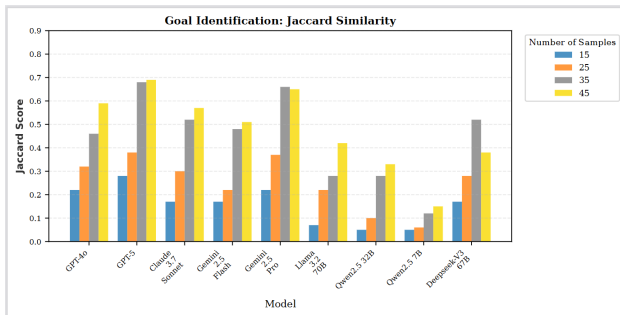


Figure 22. Goal Parsing Performance: Jaccard similarity scores across different models and sample sizes. Goal parsing assesses the precision of identifying the problem’s objective. All metrics use fuzzy matching as described in Section 6.3.1.

outperform open-source models, with larger models showing better performance within the same model family. The Parse Score effectively captures overall parsing quality by equally weighting the three components, ensuring comprehensive parsing capability is rewarded.

C.4. Prompt Templates

This section introduces the specific prompt templates used in the M2FP system for CDL parsing and direct problem solving. The M2FP system uses prompt engineering to guide large language models: (1) task description with role definition and schema compliance, (2) strict predicate vocabulary constraints from GDL, (3) few-shot examples covering all predicate types, (4) rule-based guidance for source separation and formatting, and (5) error prevention warnings. This approach balances flexibility with strict constraints to ensure output quality.

C.4.1. CDL Parsing Prompt Template

The following prompt template is used for **CDL parsing**, which guides large language models to convert natural lan-

guage geometric problem descriptions and visual diagrams into formal CDL representations. Parsing step starts with a targeted prompt engineering approach: specialized prompts are constructed using expertly designed example sets that cover all basic predicates. These examples can express predicates and formal language without involving complex geometric relationships, and each includes geometric descriptions and their corresponding formalizations.

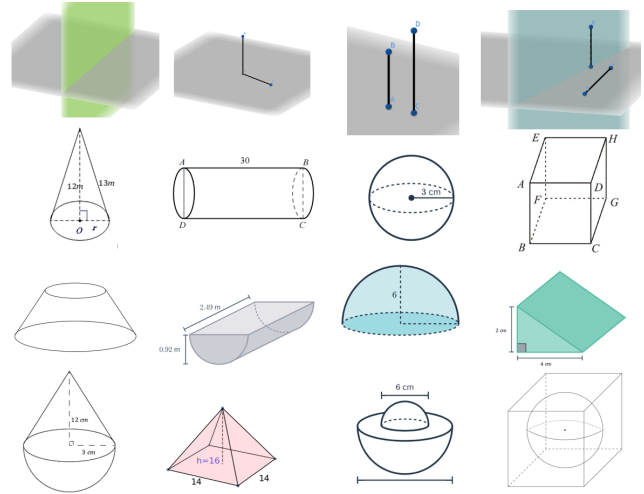


Figure 23. Examples from designed samples

The complete prompt template is shown below:

You are an expert in geometry, logic, and computer science. Your task is to precisely convert a geometry problem (with natural language and an image) into a JSON object following the provided JSON Schema. You must strictly follow the schema and output a complete JSON object.

Rule 0: Predicate Compliance (MOST IMPORTANT)

- All CDL predicates you generate (e.g., Equal, Cone, LengthOfLine) MUST be strictly chosen from the official list below.
- Using any predicate that does not appear in this list is strictly forbidden.

```
--- Official Predicate List ---
[valid_predicates_str]
--- End of Official Predicate List ---
```

Core Rules and Constraints:

1) Information Source Separation:

- text_cdl MUST include only facts extracted from the natural language description.
- image_cdl MUST include only facts directly observable from the image (e.g., length labels, right-angle marks, shape recognition).
- If a fact appears in both text and image, include it in both fields.

2) construction_cdl - Geometric construction predicates (IMPORTANT): construction_cdl defines basic construction for entities, and MUST include the following types where applicable:

- Shape predicates: define edges/segments of shapes
 - * For segments/edges: Shape(AB,BC,CD,DA) or Shape(OP,PO) or Shape(PQ,QP)
 - * For points (spheres etc.): Shape(O) or Shape(P)
 - * Example: rectangles require Shape(AB,BC,CD,DA); cylinders require Shape(PQ,QP)
- Collinearity/Cocircular/Coplanar/Cospherical:
 - * Collinear(PABQ) - P, A, B, Q are collinear
 - * Cocircular(O) - O is on a circle (for cone/cylinder base center)
 - * Coplanar(U,ABCD) - U coplanar with ABCD
 - * Cospherical(O) - O is on a sphere (for spheres)

Important:

- Carefully analyze the image to identify all necessary edges/segments/relations
- Most problems require at least one Shape(...)
- Cones/cylinders often need Shape(...) and Cocircular(...)
- Spheres often need Shape(O) and Cospherical(O)

3) Answer formatting:

- problem_answer MUST be a pure number or expression (e.g., "10", "36*pi"), and MUST NOT contain units or extra text.

4) Core predicate logic:

- Length/Height:
 - Equal(LengthOfLine(A,B),5),
 - Equal(HeightOfCone(O,P),12)
- Relations:
 - PerpendicularBetweenLine(A,B,C,D),
 - ParallelBetweenLine(A,B,C,D)
- Goal: the requested quantity MUST be wrapped by Value(...).

5) Predicate and Operator Legality (CRITICAL):

- Only reuse names from the official predicate list; DO NOT invent new construction predicates.
- Quantities allowed in CDL expressions are LIMITED to standard forms: VolumeOfCone, SurfaceAreaOfCylinder, AreaOfCircle, LengthOfLine, etc.
- Only the following algebraic operators are allowed: Value, Add, Sub, Mul, Div.
- Formatting: NO extra spaces inside any predicate/operator.

6) Completeness Checks:

- Ensure every entity used by text_cdl/image_cdl exists in construction_cdl
- Ensure the target entity in goal_cdl exists in the construction as well
- Self-check after generation: verify all predicates/operators are allowed, no extra spaces, and no undeclared entities are referenced.

Important: Output Requirements

1. You MUST output a complete JSON object with all required fields
2. All CDL fields MUST be arrays of strings
3. goal_cdl MUST be a string (e.g., "Value(VolumeOfCone(O,P))")

C.4.2. Direct Problem Solving Prompt

In addition to CDL generation, the system also supports **direct problem solving** using GPT models for **testing model accuracy**. This approach bypasses formalization and directly generates answers to geometry problems, providing a baseline for comparison with formalized CDL-based reasoning systems.

The direct solving prompt is simpler than CDL generation and focuses on step-by-step reasoning. The prompt template is:

You are an expert in geometry and mathematics. Please solve the following geometry problem step by step.

Important Instructions:

1. Carefully analyze the problem text and the accompanying image
2. Show your reasoning process step by step
3. At the end, provide your final answer in a clear format
4. ****Your final answer should be ONLY a number or mathematical expression (like "10", "5.5", "12*pi", "36*pi"), without any units or text****
5. Put your final answer on a line starting with "FINAL ANSWER: "

Example format:

FINAL ANSWER: 10

or

FINAL ANSWER: 36π

Now, please solve this problem:

D. SGRE Supplementary Information

D.1. Theorem Search Tree and Search Process

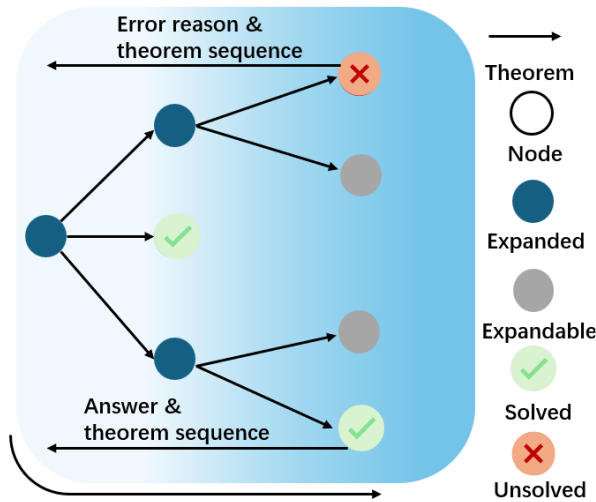


Figure 24. Theorem Search Tree and a inference demonstration is shown in fig. 28

The search process involves constructing a search tree, where nodes represent a set of known conditions, this constitutes a state variable, while arrows denote the applied theorems that supplement the existing 0 condition. As shown in figure 24, starting from the known conditions of the problem, theorems are continuously applied to derive new conditions until the goal is reached. The search tree is traversed using either breadth-first or depth-first search, returning nodes in the "expandable" state. The theorems associated with the current nodes are then repeatedly applied to verify if the problem has been solved. Guided by the known conditions of the current node, the "expand" operation checks the list of applicable theorems and generates new nodes. A simple example of "expand" is as follows: given a cube with a known side length, it is intuitive to expand to other side lengths and various angles. This process requires no additional theorem application and can also validate contradictory conditions resulting from upstream parsing.

D.2. Traditional Search vs. SGRE

Traditional search has various optimization schemes, such as heuristics, but simple pruning of search is not the focus of this paper. The traditional search focuses only on "inferring the target from the known". In contrast, SGRE draws inspiration from SMT (Satisfiability Modulo Theories), which not only determines satisfiability and proactively identifies contradictions but also addresses multi-constraint conflicts (e.g., given a cube with two known distinct side lengths, it

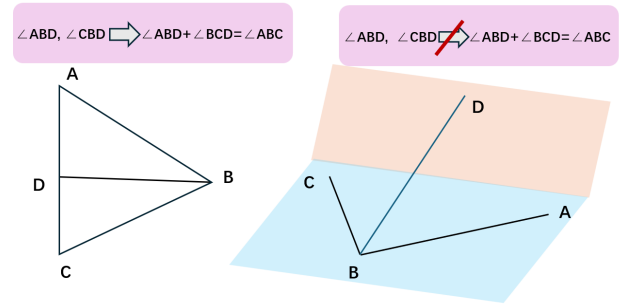


Figure 25. Plane and Solid differ greatly in all aspects, even if the CDL is consistent. SGRE needs to distinguish the Combination of multiple theories

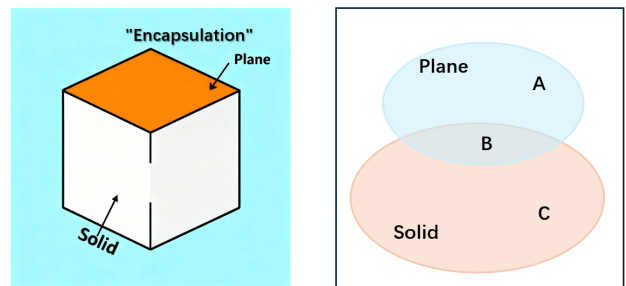


Figure 26. Regarding the encapsulation of the planar theorem, Coplanar(point_seqs) will be treated as a Plane class to apply the theorems and "extend" in set A (See Fig. 27)

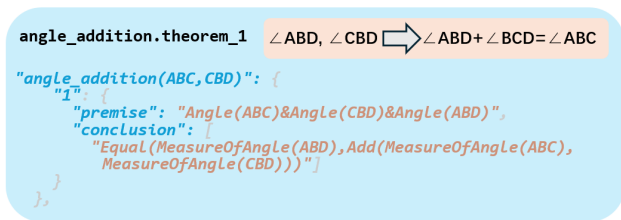


Figure 27. A theorem (as illustrated in Fig. 25) that falls into set A holds true exclusively within the Plane Class

returns "unsatisfiable" and provides the cause of the conflict—specifically, the contradictory constraints) and combinations of multiple theories (e.g., hierarchical rapid evaluation of planar and solid properties: the constraints required for problem-solving vary under different theoretical frameworks; see Figure 25). This demonstrates the feasibility of subsequent integration between Hilbert-Geo and large-scale mathematical tools.

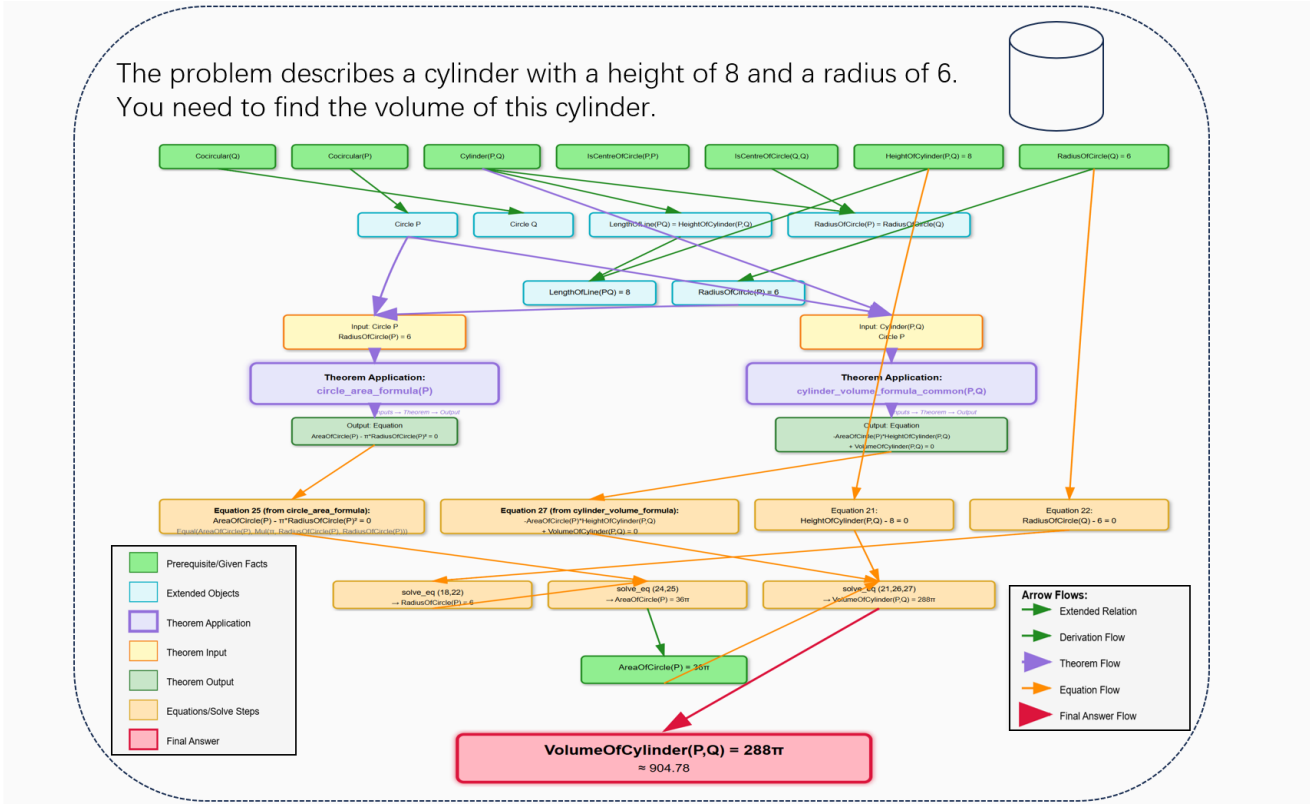


Figure 28. one illustrative example for reasoning based on Hilbert-Geo

E. Experiments

This section supplements some content to the experimental part.

E.1. Mathverse-solid

The findings in Table 9 underscore the inherent challenges of Solid Geometry. GPT-5 emerges as the top-performing model with an overall accuracy of 62.9%, followed by Gemini 2.5 pro at 59.7% and Claude-3.7-Sonnet at 54.7%. Notably, all other models score below 50%, highlighting the significant hurdles that solid geometry reasoning presents even for cutting-edge large language models.

Notable performance disparities persist among state-of-the-art models across fine-grained tasks requiring robust reasoning. GPT-5 leads in SMR with a 67.1% score yet falls short in SSI, managing only 52.9%. Open-source models, exemplified by Deepseek-V3 67B (39.1% in CSS and 34.7% in SSI), consistently underperform relative to closed-source alternatives. Critically, all these models remain far behind human performance, underscoring the current challenges in replicating human-level solid geometry reasoning. Hilbert-Geo, by contrast, delivers a distinct perfor-

Table 9. MLLMs and Hilbert-Geo (Gemini-2.5-pro 45 samples) performances on Mathverse-solid; Four fine grains: Composite Solid Structures (CSS), Spatial Metric Relations (SMR), Solid Shape Identification (SSI), Measurement of Solid Geometric Forms (MSGF); The underline represents the best performance of MLLMs

| Model | Overall.Avg | CSS | SMR | SSI | MSGF |
|-------------------------------------|-------------|-------------|-------------|-------------|-------------|
| Closed-source MLLMs | | | | | |
| GPT-4o | 42.4 | 45.1 | 36.6 | 44.2 | 46.7 |
| GPT-5 | <u>62.9</u> | <u>64.9</u> | <u>67.1</u> | 52.9 | 56.1 |
| Claude 3.7 Sonnet | 54.7 | 57.2 | 55.3 | 50.6 | 52.4 |
| Gemini 2.5 Flash | 47.5 | 50.1 | 47.2 | 44.5 | 45.9 |
| Gemini 2.5 Pro | 59.7 | 60.6 | 61.9 | <u>54.1</u> | <u>60.1</u> |
| Open-source MLLMs | | | | | |
| Llama 3.3 70B | 36.0 | 38.2 | 36.5 | 33.8 | 33.1 |
| Qwen2.5-VL-Instruct-32B | 31.0 | 33.9 | 29.1 | 29.8 | 30.4 |
| Qwen2.5-VL-Instruct-7B | 22.9 | 24.7 | 20.4 | 23.5 | 24.2 |
| Deepseek-V3 67B | 35.4 | 39.1 | 33.7 | 34.7 | 32.2 |
| Human Performances | | | | | |
| Human | 92.1 | 93.0 | 89.4 | 97.8 | 88.5 |
| Hilbert-Geo | | | | | |
| Hilbert-Geo (Ground-Truth) (Ours) | 86.3 | 87.5 | 87.1 | 86.9 | 81.1 |
| Hilbert-Geo (Gemini-2.5-Pro) (Ours) | 84.1 | 85.9 | 84.9 | 80.2 | 78.3 |

mance profile. Evaluated on Hilbert-Geo with 45 samples, it achieves top-tier results across all key dimensions: 85.9% in CSS, 84.9% in SMR, 80.2% in SSI, 78.3% in MSGF, and an overall accuracy of 84.1%.

As shown in table 10 and figure 29. Based on Hilbert-Geo, the reasoning success rates of Gemini 2.5 Pro and GPT-5 rise sharply as the number of samples increases, approaching 90% when the sample size reaches 45. In contrast, open-source models such as Llama 3.2 70B exhibit a modest upward trend in performance, which also remains

significantly lower than that of closed-source counterparts overall.

Table 10. Performance of Different Models on Hilbert-Geo (45 Samples): Accuracy, Average Time per Solved Problem, and Reasoning Steps; The underline represents the best performance of Hilbert-Geo

| Model | Overall.Avg | CSS | SMR | SSI | MSGF |
|--------------------------------|-------------|-------------|-------------|-------------|-------------|
| Closed-source MLLMs | | | | | |
| Hilbert-Geo (GPT-4o) | 62.1 | 65.1 | 59.6 | 64.2 | 59.1 |
| Hilbert-Geo (GPT-5) | 80.5 | 84.2 | 77.1 | <u>82.9</u> | 77.5 |
| Hilbert-Geo (Claude 3.7) | 73.2 | 76.2 | 69.8 | 74.6 | 72.4 |
| Hilbert-Geo (Gemini 2.5 Flash) | 69.1 | 70.1 | 67.5 | 71.5 | 67.9 |
| Hilbert-Geo (Gemini 2.5 Pro) | 84.1 | <u>85.9</u> | <u>84.9</u> | 80.2 | <u>78.3</u> |
| Open-source MLLMs | | | | | |
| Hilbert-Geo (Llama 3.3 70B) | 52.0 | 54.6 | 46.5 | 53.8 | 56.1 |
| Hilbert-Geo (Qwen2.5-VL-32B) | 38.7 | 43.9 | 36.1 | 35.8 | 36.4 |
| Hilbert-Geo (Qwen2.5-VL-7B) | 29.4 | 30.4 | 26.9 | 33.7 | 28.2 |
| Hilbert-Geo (Deepseek-) | 46.6 | 49.1 | 44.7 | 44.7 | 47.2 |
| Formal Language Ground Truth | | | | | |
| Hilbert-Geo (CDL) | 86.1 | 87.5 | 87.1 | 86.9 | 81.1 |

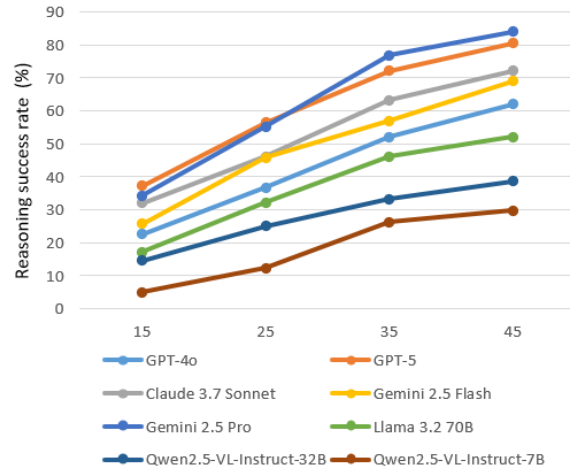


Figure 29. Reasoning performance of MLLMs under different numbers of samples based on Hilbert-Geo

E.2. PlaneFGeo3k

Table 11. MLLMs and Hilbert-Geo (Gemini-2.5-pro 45 samples) performances on PlaneFGeo3k

| Model | Accuracy (%) |
|-------------------------|--------------|
| GPT-4o | 47.2 |
| GPT-5 | 68.1 |
| Claude 3.7 Sonnet | 60.0 |
| Gemini 2.5 Flash | 55.6 |
| Gemini 2.5 Pro | 72.3 |
| Llama 3.2 70B | 33.3 |
| Qwen2.5-VL-Instruct-32B | 24.8 |
| Qwen2.5-VL-Instruct-7B | 17.5 |
| Deepseek-V3 67B | 30.4 |
| human | 87.9 |
| Ground Truth | 84.1 |
| Hilbert-Geo | 80.2 |

As shown in table 11, GPT-5 emerges as the top performer with an overall accuracy of 72.3%, followed by Gemini 2.5 Pro at 68.1% and Claude 3.7 Sonnet at 60.0%. Notable performance disparities persist among leading models. Open-source models like Llama 3.2 70B consistently underperform compared to closed-source ones. Critically, all these models remain far behind human performance, highlighting the current difficulties in replicating human-level plane geometry reasoning. Hilbert-Geo, by contrast, delivers a distinct performance profile. Evaluated on Plane-Geo with 45 samples, it achieves excellent results across all key areas, with an overall accuracy of 80.2%.